Organic Carbon Burial Rates in Mangrove Soils: Global Context and A preliminary Investigation of the Coastal Everglades

by

Joshua L. Breithaupt

A thesis submitted in partial fulfillment
Of the requirements for the degree of
Master of Science
Department of Environmental Science & Policy
College of Arts and Sciences
University of South Florida St. Petersburg

Co-Major Professor: Joseph M. Smoak, Ph.D.
Co-Major Professor: Thomas J. Smith, III, Ph.D.
Kathleen Carvalho-Knighton, Ph.D.
Armando Hoare, Ph.D.

Date of Approval:
July 2, 2012

Keywords: mangroves, organic carbon, carbon burial, blue carbon, Everglades, coastal wetlands

Dedication

To Rachel, Murray, & Miles.

Acknowledgements

I thank my committee members for guiding, listening, questioning and directing through the various stages of this research. I also wish to thank Dr. Christian Sanders of the Universidade Federal Fluminense, Brazil for his advice and insights that have provided much of the foundation for this work.

I am thankful for field sampling assistance from Gordon Anderson and Paul Nelson of the US Geological Survey, and to University of South Florida students Marietta Mayo, Miranda Oliver, and Tom Harmon for their help processing samples in the laboratory.

Discussions with faculty and students involved in the Florida Coastal Everglades Longterm Ecological Research program (supported by the National Science Foundation under Grant No. DBI-0620409) are gratefully acknowledged. I thank the FCE LTER for awarding me a Spring 2012 Travel Grant by which I was able to share this research at the 9th INTECOL International Wetlands Conference.

Table of Contents

List of Tables

List of Figures

Abstract

The ecological and economic contributions made by mangroves have been well documented in recent decades, and these coastal forests have been the focus of increased attention in terms of conservation and restoration. One aspect that has recently drawn increased attention is the role of mangrove environments in the global carbon cycle, particularly for their high burial rates of organic carbon (OC), also known as "Blue Carbon", that would otherwise contribute to increased atmospheric CO_2 levels. Globally, the amount of available data has more than doubled since the last primary literature review of OC burial in mangrove sediments (2003). The objective of this research is to recalculate the centennial-scale burial rate of OC at both the local and global scales. Quantification of this rate enables better understanding of the current carbon sink capacity of mangroves, as well as helping to quantify and/or validate the other aspects of the mangrove carbon budget such as import, export, and remineralization. Our estimate is that mangrove systems bury 163 (+39.2; -32) g OC m^{-2} yr^{-1}. Globally, the annual burial rate is 26.1 (+6.3; -5.1) Tg OC. This represents 10-15% of estimated annual mangrove production and supports previous conclusions that, on a centennial timescale, 8 to 15% of all OC burial in marine settings occurs in mangrove systems.

The second objective of this research is to provide direct measurements of spatio-temporal differences in OC burial rates at a high-productivity mangrove forest near the mouth of the Shark River in Everglades National Park. The burial rate of OC was determined via radiometric dating (i.e. ^{210}Pb) of six soil cores taken at distances ranging

from 25 – 170 m from the Shark River. The resulting mean OC burial rate for the site is 124 g m^{-2} yr^{-1}, considerably lower than the global estimate. When compared with the local production estimate, the OC burial fraction ranges from 8 to 12% over the course of a century. While the accumulation rate of inorganic matter generally decreases with distance from open water, the OC burial rates show much less predictability, indicating the influence of different controlling mechanisms. Additionally, each core demonstrates a signature of influence from hurricane Wilma (2005). The enhancement of both OC burial and soil surface accretion rates offer evidence of positive hurricane impacts that need to be balanced with assessment of the destructive contributions such as tree mortality and erosion.

Chapter 1:

Organic Carbon Burial Rates in Mangrove Sediments: Strengthening the Global Budget

Introduction

Mangrove systems research has increasingly focused on carbon cycle dynamics and sequestration in the last twenty years (Table 1). Situated within the transition zone between terrestrial and marine environments, these wetlands provide a unique combination of both organic matter production and sequestration. The global extent of mangrove sediment surface area is less than 2% of the area of marine environments, yet they are estimated to account for 10 to 15% of the total OC burial in marine environments [Duarte et al., 2005; Jennerjahn and Ittekot, 2002]. The sink function occurs in mangroves if the rate of carbon entry to a system via photosynthetic transformation to plant and eventually sediment material, is greater than the rate at which it leaves via export or respiration [Twilley et al., 1992]. Two inter-related measurements of importance to this sequestration are the sediment OC density and the OC burial rate. The first informs measurements of the stock currently secluded from the atmosphere and has been addressed at length in recent years [Duarte et al., 2005; Bouillon et al., 2008], with estimates that up to half of mangrove sequestered carbon is found in the sediments [Donato et al., 2011]. Measurement of the burial rates addresses the question of how much carbon is stocked in a specified time period and is the focus of this review. The rate

measurement enables quantification of the ongoing sink capacity, and subsequently helps to quantify and/or validate the other aspects of a system-scale carbon budget such as import, export, and remineralization.

Conversely, the standing stock and burial rate of OC also contribute to understanding potential consequences if the sink capacity is compromised. Much attention has been given to the responses of mangroves to global climate change and the potential impact of rising sea levels, altered precipitation patterns, elevated atmospheric CO_2, and changing temperatures [Gilman et al., 2008; Alongi 2008; McKee and Rooth, 2008]. System responses are not expected to be uniformly positive or negative in all mangrove settings. Each factor has the potential to direct changes in the rates of production, burial, export or decomposition of the organic matter. Sea level is perhaps the most immediate concern because if mangal sediment surface level does not maintain at least an even pace with the changing sea level, the system's sink capacity may be compromised and the buried organic matter exposed to conditions favorable to decomposition and remineralization to gaseous form [Gilman et al. 2007; Barr et al., 2011]. Organic carbon burial in some environments, especially those with a lack of regular allochthonous sediment input to build sediment surface levels, has been shown to balance a sediment accretion deficit compared to sea level through peat creation and subsequent sediment surface accretion via mangrove production, particularly belowground [McKee 2011; Donato et al, 2011]. As opposed to the deleterious outcomes that may result from elevated atmospheric CO_2, there are indications from salt marshes that elevated atmospheric CO_2 and water salinity (influenced by both precipitation and sea-level), can have a positive impact on belowground production and contribute to

increased sediment elevation levels [Langley et al., 2009]. In general, before broad considerations of these responses can be examined, it is necessary to establish a firm understanding of current burial rates and the spatio-temporal influences.

The concentration of OC present at any sediment depth will depend on the processes of delivery and degradation over time [Zimmerman & Canuel, 2000]. Therefore, OC burial rates are measured based on the OC presently available for measurement and not the amount originally deposited. Thus, determination of mean OC burial rates is partially dependent on the timescale of interest, and consequently on the dating methods used to measure sediment accumulation rates. These assumptions, along with consideration of the time scale at which recent global climate change occurs, contribute to the objectives of this study which is to focus on burial rates derived from dating methods working at the centennial scale such as ^{210}Pb and ^{137}Cs. Two other common methods for dating sediment accumulation rates in wetlands have been excluded because of their operation on different time scales. First, although ^{14}C has been widely used for the dating of entire mangrove peat profiles [Jennerjahn and Ittekot, 2002 and references therein; Eong 1993; Twilley et al., 1992 and references therein], it works on a millennial scale and thus falls outside the scope of our focus on centennial scale processes. Secondly, for measurement on small timescales in salt marshes and some mangrove systems, repeated measurements of sediment accumulation above a marker horizon have contributed to measuring sub-annual rates [e.g. Cahoon and Lynch, 1997]. However, storage of OC at the surface level is not the same as longer-term burial as up to 97% of this may be lost to diagenesis within the first year of deposition [Duarte and

Cebrian 1996] and therefore rates derived from surface marker horizons have also been excluded from consideration in this review.

There have been five review papers in the past two decades that, as part of their scope, have included some consideration of largely centennial-scale OC burial rates in mangrove sediments (Table 1). As was noted by Bouillon et al. [2008] each of these has taken a slightly different approach. Both Twilley et al. [1992], and Chmura et al. [2003] considered primary research literature values of direct measurements to determine mean global annual burial rates. Jennerjahn & Ittekkot [2002] utilized a mass balance approach and available estimates of production, litterfall, export and remineralization to estimate that 25% of mangrove litterfall is sequestered in the sediment annually. Chmura et al. [2003] have provided the most recent thorough compilation of directly measured century-scale burial rates in mangrove systems. They used a sample number of 28 taken from five sites in three countries to determine an arithmetic mean burial rate of 210 g OC m^{-2} yr^{-1}. In 2005 Duarte et al. utilized the dataset from Chmura et al. [2003], but recalculated the average using a geometric mean (139 g OC m^{-2} yr^{-1}) due to the skewed nature of the dataset. In addition to these previous studies that have provided in depth reviews of the literature and methods, there have been at least two references in recent years that have advocated revision of the mean global burial rate, but without providing a methodological discussion. Alongi [2009] proposed altering the values of Duarte et al. [2005] upward to 181.3 g OC m^{-2} yr^{-1} at the local level, and 29.0 Tg OC yr^{-1} at the global level. Mcleod et al. [2011] suggested an upward revision to 226 ± 39 g OC m^{-2} yr^{-1} at the local scale, and, because of different methods and conclusions used for estimating the global areal extent of mangrove forests, provide a range of global rates from 31.1 ± 5.4 to 34.4 ± 5.9 Tg OC

yr^{-1}. It is especially important to note the different areal extent of mangrove forests referenced in these studies as its use in up- or downscaling contributes to substantial differences. It is therefore useful to standardize the burial rates to a common areal extent for comparison. Here (Table 1) we have used a value of 1.6×10^{11} m^{-2} [FAO, 2003] to maintain consistency and compatibility with the other carbon pools in the most recent discussion of a global mangrove carbon budget [Bouillon et al., 2008].

Because a considerable amount of new data has been collected since the last detailed assessment of direct measurements, the objective of this study is to strengthen the global mangrove carbon budget by recalculating the central tendency of the measured rates of centennial-scale OC burial in mangrove systems. Additionally, we separately consider un-forested locations immediately adjacent to mangrove forests such as tidal flats and lagoons. It is important to differentiate these locations because estimates of the global areal extent of mangrove forests (which do not include mudflats, bays or lagoons) are used when up-scaling local to global burial rates.

Methods

A literature review was conducted with the objective of finding direct measurement research utilizing ^{210}Pb or ^{137}Cs to quantify OC burial rates in mangrove systems. Where data was provided regarding the sediment OC percentage and sediment mass accumulation rates, these values were used to calculate a burial rate even if the stated objective of the research was to measure something other than OC burial rates. Study locations were noted, along with details regarding site characteristics including mangrove species predominance and forest type when provided. Quantitative data

objectives included local burial rates, sediment accretion rates, sediment OC density, and primary production rates. Production rates are not frequently considered in the primary research literature, but do play an important role in secondary literature when considering the various components of the carbon budget. Qualitative data objectives sought included the rate measurement method, use of elemental ratios or stable isotope concentrations, riverine influence, and site location coordinates. Core dimensions were also recorded.

Whenever possible individual core records were used, and when necessary means were calculated from tables or figures. If a paper reported only the range of mean burial rates for multiple cores but not a mean value for individual cores, then only the upper and lower values were used here [e.g Tateda et al., 2005]. Additionally, in the event that a range of burial rates was given for a single core, the mid-point of the two values was used as a functional mean [e.g. Ruiz-Fernandez et al., 2011]. All data were recalculated with the intent of reproducing the research's stated results to provide an internal check on our statement of burial values. When organic matter (OM) was reported, that value was multiplied by 0.58 after Allen [1974] to estimate the OC content. When individual core rates were not provided, they were calculated by multiplying mass accumulation rates by the percentage of OC present [e.g. Alongi et al., 2005]. When necessary, units were converted for consistency in comparisons.

In previous reviews there has been some disagreement about whether to use the arithmetic or geometric mean [Chmura et al., 2003; Duarte et al., 2005] with substantial global differences (Table 1). A Normal Univariate Procedure was used to analyze the distribution as well as the skewness and kurtosis of the data (SAS Institute, Cary, North Carolina, USA). Shapiro-Wilk test results provided an indication of normality for the

regular and log-transformed versions of the data to determine whether the central tendency is best represented by the arithmetic mean, geometric mean, or median.

Results

Nineteen studies were found with data related to the centennial-scale burial of OC in or near mangrove systems (Table 2). Considerable amounts of primary research have been conducted in the past decade since the last review [Chmura et al., 2003]. Representation is now included for Brazil, Columbia, Malaysia, Indonesia, China, Japan, Vietnam, and Thailand, along with additional data from Mexico and the United States. The primary dataset consists of 65 individual sediment cores (Table 2A). An additional smaller dataset is provided from 9 cores retrieved in areas adjacent to mangrove forests such as a tidal mudflat or bordering lagoon (Table 2B).

Of the 65 cores in the primary dataset, 22 were referenced in Chmura et al. [2003]. Four of their other data points were excluded from this study for methodological reasons. The work of Cahoon and Lynch [1997] represents short-term (1-2 years) surface accumulation rates measured with horizon markers, and as was discussed earlier, these shorter-term rates fall outside the objectives of this study. Additionally, two cores from Australia [Alongi et al., 1999] were retrieved from mudflats and were removed from our primary dataset to that of adjacent systems (Table 2B).

There is a large range of burial rates within the forested sites (Table 2A), from 22 (Fukido, Japan) to 1,020 g OC m^{-2} yr^{-1} (Jiulongjiang Estuary, China). Accompanying this global variability, local ranges can be similarly pronounced. In Hinchinbrook Channel, Australia, the rates range from 26 to 336 g OC m^{-2} yr^{-1}, and in the Jiulongjiang Estuary of

China, the rates range from 168 to 841 g OC m^{-2} yr^{-1}. There are also locations where much less variability is represented. In Rookery Bay, Florida, Lynch [1989] found a range of only 69 to 99 in 4 cores, and in Sawi Bay, Thailand, Alongi et al. [2001] found a range of 184 to 281 g OC m^{-2} yr^{-1}.

The arithmetic mean is 231 ± 209 g OC m^{-2} yr^{-1}. The large error should not obscure the increase over the previous estimate of 210 g OC m^{-2} yr^{-1} (without error estimation) in the last review of primary research by Chmura et al. [2003]. This arithmetic mean is very similar to the Mcleod et al. [2011] estimate of 226 ± 29 g OC m^{-2} yr^{-1}. Because no discussion of methods for calculating their error are provided we are unable to determine the reason for the substantial difference with the estimated errors found in this study. However, the untransformed data have a right skew, a heavy right tail, and a strong indication of not coming from a Normal probability distribution (p-value < 0.0001, see Table 3). Similar results were found for the 5% and 10% trimmed arithmetic means, indicating that the non-normality of the dataset is not due simply to a few upper and lower outliers. The results show that the log-transformed values provide the greatest indication of coming from a Normal probability distribution (Shapiro Wilk p = 0.2699) and therefore the geometric mean is used here as the most representative measure of central tendency. The geometric mean of these data is 163.3 (+39.2; -32) g OC m^{-2} yr^{-1}; the 95% confidence interval is from 131.3 to 202.5 g OC m^{-2} yr^{-1}.

We have chosen to separate the data retrieved from locations adjacent to the margins of mangrove forests. There is an even larger range of burial rates with this adjacent dataset, from 5 (Florida, USA) to 1129 g OC m^{-2} yr^{-1} (Tamandare, Brazil). The data from these cores were shown to come from a Normal distribution (Shapiro Wilk p =

0.0594), however this is not unexpected with such a small sample size (n=9). Because the larger dataset has been shown to represent a Normal distribution when the values are log-transformed, that approach was taken with this adjacent system dataset as well (Shapiro Wilk p = 0.2431). The geometric mean is 158.6 g OC m^{-2} yr^{-1} and the 95% confidence interval is from 41.6 to 605.3 g OC m^{-2} yr^{-1}.

When available, the sediment accretion rates and the mean sediment OC% were obtained for cores and subjected to the same Normal Univariate procedure (SAS 9.2). The outcomes of these tests are provided in Table 3. The median was determined to be the most appropriate indication of central tendency for both categories. The median accretion rate is 2.8 mm yr^{-1} with a 95% confidence interval of 1.9 to 3.9 mm yr^{-1}. The median sediment %OC is 7.0 with a 95% confidence interval of 4.3 to 14.4%.

Discussion

Burial rates and considerations of primary production

We have provided statistical analysis of the data's distribution because small differences in the local level burial rates become more pronounced when raised to the global scale. Here, the local scale difference between geometric and arithmetic means of 68 g OC m^{-2} yr^{-1} equates to 10.9 Tg OC yr^{-1} globally. The evidence supports use of the geometric mean, and the added precision enables better understanding of both the quantification and direction of carbon cycling pathways. Bouillon et al. [2008] calculated a global mangrove production rate of 218 ± 72 Tg C yr^{-1} including an OC burial rate of 18.4 Tg yr^{-1}. Note that this is the global scale burial rate derived by up-scaling the geometric mean from Duarte et al. [2005], which was modified from Chmura et al.

[2003]. Using the geometric mean derived here, the revised estimate of annual burial rates is 26.1 Tg OC, a 42% increase and an annual difference of 7.7 Tg (Table 1). When the errors are raised to the global scale, the range of possible burial rates is 21.0 to 32.4 Tg yr^{-1}. Accordingly, OC burial equates to an expected range of 9.6 to 14.9% of estimated global annual mangrove production (Figure 1). This range should not be thought to imply that all of the buried OC originates with mangroves. Rather, the OC buried in mangrove sediments may include material imported from both marine and terrestrial environments. With this revision, rather than being the smallest fractional fate of production, burial is roughly equivalent to the export fractions of dissolved and particulate OC. The two largest pools continue to be CO_2 efflux and the unaccounted portion (Figure 1). Note also that the difference between geometric and arithmetic means of 10.9 Tg yr^{-1} mentioned above, is 5% of production and would constitute a substantial error.

Organic Matter Origins & Delineation of Mangrove Extents

All sources of production and input need to be identified and accounted for in order to accurately measure burial as a percentage of production, and similarly the buried OC needs to be fractioned according to its point of origin. Locations with high rates of input from riverine or tidal sources can experience increased rates of OC burial in addition to that provided by autochthonous production [Jennerjahn and Ittekot, 2002]. For example, Alongi et al. [1998] note that mangrove carbon represented only 56% of the total OC input to Hinchinbrook Channel, and Gonneea et al. [2004] note widely varying contributions of mangrove material over time in different coring locations. It would be

inaccurate to attribute all the buried OC to mangroves, and would overstate the burial fraction of overall production.

A primary reason for the end-member analysis is to correctly allocate buried OC to its production origins, whether they be terrestrial, marine, or mangrove. The longstanding estimates of total marine OC burial have ranged from 126 to 160 Tg yr^{-1} [Berner, 1982; Hedges & Keil, 1995]. However, in 2005 Duarte et al. nearly doubled the values of total OC buried in marine sediments to a range of 216 to 244 Tg yr^{-1}, in order to account for burial within marginal vegetated habitats of sea grass, salt marsh and mangroves. Correcting for the values used in this review for areal extent (1.6×10^{11} m^2) and annual burial rate (26.1 (+6.3; -5.1) Tg OC yr^{-1}) the estimate of annual marine OC burial should range between 213.7 and 252.4 Tg. Based on this range, our estimate for the mangrove fraction of the total annual marine burial rate ranges from 8.3 to 15%. This is in good agreement with the percentages estimated by Jennerjahn & Ittekot [2002] and Duarte et al. [2005] despite different approaches and different local scale burial rates, and emphasizes the importance of these coastal systems. As wetland systems that are often overlooked in both terrestrial and marine contexts, current data demonstrate that mangroves are both producing and burying more OC than has previously been recognized. These data emphasize the need for more end-member analyses to characterize the composition of OM burial rates to account for the OC that may be attributed to mangrove, as well as terrestrial and marine production.

We have given specific consideration to a smaller subset of data taken from sediments that are near, but not within, mangrove forests. Three study locations provide data both from within the mangrove system and the adjacent settings, allowing for local

comparison. In Australia [Alongi et al., 1999] and Brazil [Sanders et al., 2010b] there are no differences in OC burial rates between forested and un-forested sediments. A third study at Celestun Lagoon in Mexico [Gonneea et al., 2004] is more complicated because of the extensive analysis of organic matter provenance using C:N ratios and stable isotopes. The burial rate within the lagoon was slightly lower than the two cores taken within the forest margins (40 vs. 55 & 70 g OC m^{-2} yr^{-1}) in terms of total organic carbon (TOC). However, the provenance analysis enables isolation of the specifically mangrove organic carbon (MOC) burial rate, and here the differences are notably different. The forest burial rate of MOC was between 20-60 percent of the TOC burial rate for Station 6, and between 60-70 percent for Station 16 (with the exception of a near-surface low of only 5% MOC). The percentage of MOC in the core from within the lagoon was between 10-25% of TOC. The authors note that their analysis reveals the temporal variability in OC contribution from mangrove, seagrass, and suspended particular matter, but that overlying vegetation is the dominant contributor [Gonneea et al., 2004].

Although MOC is being buried in the sediments of bays, mudflats, and lagoons adjacent to mangrove forests, the limited evidence presented in this review does not suggest any alteration to the expected central tendency of the global annual burial rate. Combining the values for both datasets has almost no effect on the central tendency measurement. The geometric mean remains at 163 g m^{-2} yr^{-1} and the 95% confidence interval widens slightly (129 to 205 g OC m^{-2} yr^{-1}) to account for the extreme high and low values (Table 2B). However, if future studies undertake the same analysis of OM attribution and determine that these environments bury a considerable fraction of MOC then it would no longer be sufficient to estimate the global annual rate (in Tg of OC) by

simply up-scaling to the estimated forested areal extent. In future studies, a parameter will need to be added to account for the areal extent of adjacent un-forested environments and the percentage of their annual OC burial rates that are of mangrove origin. Additionally, it is important to note that any MOC being buried in these adjacent settings is most likely not from an unidentified source pool of carbon. Rather adjacent burial rates simply identify the fate of OC drawn from the pools of dissolved and particulate OC export quantified by Bouillon et al. [2008] (Figure 1). However, because delineation of mangrove boundaries have not always been clearly addressed in the burial rate literature, it remains a possibility that the import and export of OC within these adjacent systems may not be fully accounted for.

OC Percent of Sediment & Sediment Accretion

Kristensen et al. [2008] calculated an average literature value of 2.2% sediment OC for all mangrove settings and thereby suggested that the research documenting OC burial rates is biased toward mangrove systems that are higher in sediment carbon density. Here, the median value of 7.0 % continues to indicate under-representation of low OC% systems in the global estimate. However, it is not necessarily the case that additional data from such settings would alter the global central tendency for burial rates either upwards or downwards. For example, there are data from eight cores with OC% values that are 2.2% or lower, six from the primary data and two from the adjacent settings (Tables 2A & 2B), and the burial rates for these cores range from an extreme low of 5 to an extreme high of 840.7 g OC m^{-2} yr^{-1}. Overall the sediment OC percentage

accounts for only 9% of the variation that exists in the OC burial rate, with higher burial rates being associated with lower sediment OC%.

Of the parameters used in this study, the rate of sediment accretion is the best, though weak (R^2 = 0.29), predictor of OC burial rates. If compared with the predicted global eustatic sea level rise of between 18 and 59 cm over the current century [Gilman et al., 2008] then mangrove sediments in the sites measured here are accreting only enough to keep up with the low end of the estimates, with an average surface accretion rate of 28 cm per century. If these systems should fail to keep pace, not only will their sink capacity be diminished, but the stock of OC already buried may be subject to oxidizing conditions and potentially removed back to gaseous form in the atmosphere [Bouillon, 2011]. While the fringing edges of a mangrove forest may be subject to erosion and oxidation, in some geophysical settings this may be offset by transport and re-deposition [Smoak et al., in Review, 2012] and landward migration [López-Medellín et al., 2011].

Future Research Considerations

The exercise of reviewing literature and standardizing values presents a number of challenges, and serves as a valuable measure of parameters that are currently available in the published research. Here we present a brief list of parameters that would make future reviews more robust and potentially useful for predicting global burial rates relative to local conditions.

1. There is a surprising dearth of published OC burial rates in many notable mangrove locations including all of Coastal Africa. Indeed it is easier to provide a list of places that have been sampled rather than those that have not.

For example, Central and South America is represented by Mexico and Brazil, and one lagoon core from Columbia. More effort should be undertaken to bring the many absent locations into the global estimate.

2. This review suggests that there are locations of focusing and dilution of OC burial. In addition to seeking out such coring locations, there is a general need for more spatial distribution when measuring local burial rates in order to provide a better understanding of spatial and temporal variability. Additional work should be undertaken to understand the potential of this impact relative to increased storm frequency that may accompany some regions with global climate change.
3. Similarly, as has been mentioned, these data appear biased to sediments with a higher %OC than is expected for all mangrove settings [Kristensen et al., 2008]. More measurements are needed in low OC-density settings to determine whether OC burial rates are different from the current estimate.
4. Because local conditions appear to play so prominent a role in burial rates, there is much usefulness in providing as many local traits as possible for where individual cores have been retrieved. These may include intertidal position, species predominance, forest type, hydrologic influences, geochemical conditions, regional climate traits, and level of anthropogenic influence among others.
5. It is increasingly apparent that identifying the origin of the OM is important, and future work would benefit from more analysis of this sort, whether utilizing C:N ratios, stable isotopes, or other organic tracer methods. From the

standpoint of measuring mangrove potential to mitigate elevated atmospheric CO_2 levels, the burial of any OC is a valuable ecosystem service. However if the system mass balance is not able to specifically quantify the production and burial (as well as other vectors) of mangrove OC, then the ability to quantify the sink capacity of mangroves is compromised.

Conclusion

Sequestration of carbon is a notable function in many forests, but the rates and fates of carbon flow, including biomass and burial fractions, vary with type, age, anthropogenic influence, and climate [Luyssaert et al., 2007]. Mangrove forests sequester carbon as both biomass and as organic sedimentary matter. The standing stock of these pools have recently been addressed [e.g Donato et al., 2011] and contribute to our understanding of the quantities of carbon that stand to be reintroduced to the atmosphere in the event of deforestation, sediment oxidation, or peat collapse. Here we provide a revision and constrainment of previous estimates of the century-scale burial rates derived from local direct measurements. The geometric mean global burial rate at the local scale is 163 (+39.2; -32) g OC m^{-2} yr^{-1}. At the global scale this equates to 26.1 (+6.3; -5.1) Tg OC yr^{-1}, or 8 to 15% of OC buried in all marine sediments annually. Should factors of climate change such as rising sea level and increased frequency and intensity of storms occur to such an extent that mangrove forests are stressed and unable to sequester carbon at current rates, there is risk not only that the sink capacity may be compromised, but also that the standing stock will be impacted. The result may be not only a change in sink

capacity, but possible conversion to a source, releasing even more carbon into the atmosphere.

The use of the geometric mean as a measure of central tendency has been employed because of extreme values that contribute to a heavy right-tailed, right-skewed dataset, and the natural question is whether these altering values represent anomalies, or whether they represent areas of both focused and depleted OC burial that are underrepresented in the overall sampling. Future research is required to fully answer this question. Although the available data have increased in the past decade, this is still a limited dataset in terms of global reach. At most, using the extended dataset of 74 cores (forested and un-forested sediments), if every researcher here has retrieved cores that were 20cm in diameter, our estimate of global burial rates is based on an areal coverage of 2.32 m^2, or approximately $1x10^{-8}$ % of the global areal coverage for mangroves. So while this study provides improved spatial representation over previous estimates, large geographic regions remain entirely unrepresented in these considerations. Additionally, results here suggest that there is potential for large variability even within close proximities, and indeed there appear to be locations where focused OC burial occurs at high rates. Given the uncertainties and the still large unaccounted fraction of mangrove OC production, there is a great deal of research opportunity for improving the resolution and representation of OC burial rates.

Tables

Table 1: Secondary Research Values for Local and Global Century-scale OC Burial Rates

Authors	Local Burial Rate ($g\ m^{-2}\ yr^{-1}$)	Study's Mangrove Areal Extent (km^2)	Global Burial Rate ($Tg\ C\ yr^{-1}$)	Global Burial Rate ($Tg\ C\ yr^{-1}$) (Standardized to 160,000 km^2)
Twilley et al., 1992	100	240,000	24.0	16.0
Jennerjahn & Ittekkot, 2002	115	200,000	23.0	18.4
Chmura et al., 2003	210	181,000	38.0	33.6
Duarte et al., 2005	139	200,000	27.8	22.2
Bouillon et. al., 2008	115	160,000	18.4	18.4
Alongi 2009	181	160,000	29.0	29.0
Mcleod et al., 2011	226	137,760 152,361	31.1 34.4	36.2
This Study	163	137,760 152,361	22.5 24.9	26.1

Table 2. Sediment Accretion Rates (SAR), Soil OC%, & OC Burial Rates (OC BR) of Mangrove Forest Sites (n=65)

Sampling Site	Lat.	Long.	Core ID	Riverine Presence	SAR (mm yr^{-1})	OC%	OC BR (g m^{-2} yr^{-1})	Carbon Method[b]	Dating Method	Source
Terminos Lagoon-Boca Chica	18.7N	91.5W	15m	Palizada River	4.4	10.2	237	OM	^{210}Pb & ^{137}Cs	1[a]
Terminos Lagoon-Boca Chica	18.7N	91.5W	100m	Palizada River	1.3	5.1	79	OM	^{210}Pb & ^{137}Cs	1
Terminos Lagoon-Estero Pargo	18.7N	91.5W	10m		2.9	14.6	157	OM	^{210}Pb & ^{137}Cs	1
Terminos Lagoon-Estero Pargo	18.7N	91.5W	225m		1	19.1	75	OM	^{210}Pb & ^{137}Cs	1
Celestun Lagoon, Mexico	20.8N	90.3W	6		3	7.0	55	TOC	^{210}Pb	2
Celestun Lagoon, Mexico	20.8N	90.3W	16		3	7.0	70	TOC	^{210}Pb	2
Chelem Lagoon, Mexico	21.3N	89.7W	9			4.3	85.5	TOC	^{210}Pb	2
Terminos Lagoon, Mexico	18.5N	91.8W	7			4.3	53	TOC	^{210}Pb	2
Terminos Lagoon, Mexico	18.5N	91.8W	15			4.0	65	TOC	^{210}Pb	2
Ilha Grande, Brazil	25.3S	48.3W	N/A		1.8	4.1	186	TOC	^{210}Pb	3
Tamandare, Brazil	8.7S	35.1W	T5C	Formoso River	2.8	5.8	353	TOC	^{210}Pb	4
Tamandare, Brazil	8.7S	35.1W	T5B	Formoso River	5	6.9	949	TOC	^{210}Pb	4
Cananeia, Brazil	25.3S	48.3W	C3A	Ribeira of Iguape River	2.5	3.0	192	TOC	^{210}Pb	5
Cananeia, Brazil	25.3S	48.3W	C3B	Ribeira of Iguape River	2.9	2.9	234	TOC	^{210}Pb	5
Guaratuba, Brazil	25.8S	48.7W		São João & Cubatão Rivers	2		337	OM	^{210}Pb	6
Paranagua, Brazil	25.3S	48.3W		Paranagua Estuary	2		168	OM	^{210}Pb	6
Paraty, Brazil	23.2S	44.7W			2.8		169	OM	^{210}Pb	6
Florida Keys, USA	25N	80.6W	3		4.2	32.0	209	OM	^{137}Cs	7[a]
Florida Keys, USA	25N	80.6W	6		3.9	32.0	177	OM	^{137}Cs	7
Florida Keys, USA	25N	80.6W	4		1.9	36.0	67	OM	^{137}Cs	7
Florida Keys, USA	25N	80.6W	5		1.9	36.0	91	OM	^{137}Cs	7
Florida Keys, USA	25N	80.6W	2		4.2	36.0	192	OM	^{137}Cs	7
Rookery Bay, FL, USA	26N	81.7W		Henderson Creek			20	N/A	^{210}Pb & ^{137}Cs	15
Rookery Bay, FL, USA	26N	81.7W		Henderson Creek			39	N/A	^{210}Pb & ^{137}Cs	15
Rookery Bay, FL, USA	26N	81.7W	10m	Henderson Creek	1.7	24.0	90	TOC	^{210}Pb & ^{137}Cs	1
Rookery Bay, FL, USA	26N	81.7W	30m	Henderson Creek	1.4	25.9	69	TOC	^{210}Pb & ^{137}Cs	1
Rookery Bay, FL, USA	26N	81.7W	50m	Henderson Creek	1.6	28.7	86	TOC	^{210}Pb & ^{137}Cs	1
Rookery Bay, FL, USA	26N	81.7W	70m	Henderson Creek	1.7	28.6	99	TOC	^{210}Pb & ^{137}Cs	1
Shark River, Florida, USA	25.4N	81.1W	SH3-1	Shark River	3.6	19.0	151	TOC	^{210}Pb	8
Harney River, Florida, USA	25.2N	81W	SH4-1	Harney River	2.5	30.8	168	TOC	^{210}Pb	8
Hinchinbrook Channel, Australia	18.5S	146.3E	HM2	Herbert River			67	TOC	^{210}Pb & ^{137}Cs	9[a]
Hinchinbrook Channel, Australia	18.5S	146.3E	577	Herbert River	1.8		168	TOC	^{210}Pb & ^{137}Cs	10[a]
Hinchinbrook Channel, Australia	18.5S	146.3E	582	Herbert River	1.8		84	TOC	^{210}Pb & ^{137}Cs	10
Hinchinbrook Channel, Australia	18.5S	146.3E	583	Herbert River	8.5		336	TOC	^{210}Pb & ^{137}Cs	10
Hinchinbrook Channel, Australia	18.5S	146.3E	584	Herbert River	8.5		300	TOC	^{210}Pb & ^{137}Cs	10
Hinchinbrook Channel, Australia	18.5S	146.3E	585	Herbert River	1.8		100	TOC	^{210}Pb & ^{137}Cs	10

Hinchinbrook Channel, Australia	18.5S	146.3E	576	Herbert River	1.8		26	TOC	^{210}Pb & ^{137}Cs	10
Missionary Bay, Australia	18.5S	146.3E	586		1.9		71	TOC	^{210}Pb & ^{137}Cs	10
Missionary Bay, Australia	18.5S	146.3E	587		1.9		97	TOC	^{210}Pb & ^{137}Cs	10
Matang Reserve, Malaysia	4.8N	100.5E	3175	Numerous Rivers	12.5	3.6	410	TOC	^{210}Pb & ^{137}Cs	11
Matang Reserve, Malaysia	4.8N	100.5E	3176	Numerous Rivers		3.6	148	TOC	^{210}Pb & ^{137}Cs	11
Matang Reserve, Malaysia	4.8N	100.5E	3173	Numerous Rivers		7.8	296	TOC	^{210}Pb & ^{137}Cs	11
Matang Reserve, Malaysia	4.8N	100.5E	3174	Numerous Rivers		7.8	296	TOC	^{210}Pb & ^{137}Cs	11
Matang Reserve, Malaysia	4.8N	100.5E	3171	Numerous Rivers	9.7	14.4	317	TOC	^{210}Pb & ^{137}Cs	11
Matang Reserve, Malaysia	4.8N	100.5E	3172	Numerous Rivers	9.7	14.4	389	TOC	^{210}Pb & ^{137}Cs	11
Jiulongjiang Estuary, China	24.3N	117.8E	3560	Jiulongjiang River	13.5	1.8	149	TOC	^{210}Pb & ^{137}Cs	12
Jiulongjiang Estuary, China	24.3N	117.8E	3561	Jiulongjiang River	13.5	1.8	189	TOC	^{210}Pb & ^{137}Cs	12
Jiulongjiang Estuary, China	24.3N	117.8E	3562	Jiulongjiang River		1.0	199	TOC	^{210}Pb & ^{137}Cs	12
Jiulongjiang Estuary, China	24.3N	117.8E	3563	Jiulongjiang River		1.0	216	TOC	^{210}Pb & ^{137}Cs	12
Jiulongjiang Estuary, China	24.3N	117.8E	3564	Jiulongjiang River	80	1.4	1020	TOC	^{210}Pb & ^{137}Cs	12
Jiulongjiang Estuary, China	24.3N	117.8E	3565	Jiulongjiang River	80	1.4	667	TOC	^{210}Pb & ^{137}Cs	12
Fukido, Ishigaki, Japan	24.3N	124.2E		"small river"			22	TOC	^{210}Pb	13
Fukido, Ishigaki, Japan	24.3N	124.2E		"small river"			230	TOC	^{210}Pb	13
DaLoc, ThanHoa, Vietnam	20N	106E		"high river discharge"			120	TOC	^{210}Pb	13
DaLoc, ThanHoa, Vietnam	20N	106E		"high river discharge"			180	TOC	^{210}Pb	13
Trat, Thailand	12.3N	102E		"high river discharge"			100	TOC	^{210}Pb	13
Trat, Thailand	12.3N	102E		"high river discharge"			600	TOC	^{210}Pb	13
Irian Jaya, Indonesia	4.8S	136.9E	1	Ajkwa River		12.4	558	TOC	^{210}Pb & ^{137}Cs	16
Irian Jaya, Indonesia	4.8S	136.9E	3	Ajkwa River		5.5	412	TOC	^{210}Pb & ^{137}Cs	16
Irian Jaya, Indonesia	4.8S	136.9E	4	Ajkwa River		4.9	637	TOC	^{210}Pb & ^{137}Cs	16
Irian Jaya, Indonesia	4.8S	136.9E	5	Ajkwa River		6.5	717	TOC	^{210}Pb & ^{137}Cs	16
Sawi Bay, Thailand	10.3N	99.2E	Stn S1	Khlong Sawi	1.1		226	TOC	^{210}Pb & ^{137}Cs	14
Sawi Bay, Thailand	10.3N	99.2E	Stn S2	Khlong Sawi			203	TOC	^{210}Pb & ^{137}Cs	14
Sawi Bay, Thailand	10.3N	99.2E	Stn S3	Khlong I Laet			281	TOC	^{210}Pb & ^{137}Cs	14
Sawi Bay, Thailand	10.3N	99.2E	Stn S4	Khlong I Laet			184	TOC	^{210}Pb & ^{137}Cs	14

Sources:

1) Lynch 1989, 2) Gonneea et al. 2004, 3) Sanders et al. 2008, 4) Sanders et al. 2010a, 5) Sanders et al. 2009, 6) Sanders et al. 2010b, 7) Callaway et al. 1997, 8) Smoak et al., in Review, 2012, 9)Alongi et al. 1999, 10) Brunskill et al. 2002, 11)Alongi et al. 2004, 12) Alongi et al. 2005, 13) Tateda et al. 2005, 14) Alongi et al. 2001, 15) Cahoon & Lynch Unpublished, taken from Chmura et al. 2003, 16) Brunskill et al. 2004.

[a]Indicates sources that are used in Chmura et al., 2003.

[b] TOC: Organic C measured with C analyzer. OM: Organic C derived by multiplying organic matter by 0.58.

Table 3. Sediment Accretion Rates (SAR), Soil OC%, & OC Burial Rates (OC BR) of Sites Adjacent to Mangrove Forests (n=9)

Sampling Site	Lat.	Long.	Core ID	Riverine Presence	SAR (mm yr^{-1})	OC%	OC BR (g m^{-2} yr^{-1})	Carbon Method[b]	Dating Method	Source
Dove Sound, FL, USA					1.2	0.16	5	TOC	^{210}Pb	8
Celestun Lagoon, Mexico	20.8N	90.3W	3		3.0	7	40	TOC	^{210}Pb	1
Hinchinbrook Channel, Australia	18.5S	146.3E	HMF4	Herbert River			336	TOC	^{210}Pb & ^{137}Cs	6
Hinchinbrook Channel, Australia	18.5S	146.3E	HMF3	Herbert River			48	TOC	^{210}Pb & ^{137}Cs	6[a]
Paraty, Brazil	23.2S	44.7W			4.0		270	TOC	^{210}Pb	5
Cananei, Brazil	25.3S	48.3W	C3C	Ribeira of Iguape River	3.9	2.16	234	TOC	^{210}Pb	4
Guaratuba, Brazil	25.8S	48.7W		São João & Cubatão Rivers	5.6	4.9	842	TOC	^{210}Pb	2
Tamandare, Brazil	8.7S	35.1W	T5A	Formoso River	7.3	4.85	1129	TOC	^{210}Pb	3
Soledad Lagoon, Columbia	9.3N	75.8W		Sinu River	1.5	2.69	362	OM	^{210}Pb	7

Sources:

1) Gonneea et al. 2004, 2) Sanders et al. 2006, 3) Sanders et al. 2008, 4) Sanders et al. 2010a, 5) Sanders et al. 2010b, 6)Alongi et al. 1999, 7) Ruis-Frenandez et al. 2011, 8) Harmon, T., 2011.

[a]Indicates sources that are used in Chmura et al., 2003.

[b] TOC: Organic C measured with C analyzer. OM: Organic C derived by multiplying organic matter by 0.58.

Table 4. Statistical Results of Distribution Analyses

Parameter	Adjustment	Shapiro-Wilk p-Value	Skewness	Kurtosis	Mean	SD	Use value
Burial	Unadjusted	<0.0001	1.9898	4.2719	230.9	209.0	Geometric Mean: 163.3
(g OC m^{-2} yr^{-1})	Log-transformed	0.2699	-0.2163	0.0254	2.2	0.4	95% C.I.: 131.3 to 202.5
Accretion	Unadjusted	<0.0001	4.0726	16.1152	7.7	16.9	Median: 2.8
(mm yr^{-1})	Log-transformed	<0.0001	1.6561	2.9947	0.5	0.4	95% C.I.: 1.9 to 3.9
OC%	Unadjusted	<0.0001	0.8817	-0.7718	12.8	11.9	Median: 7.0%
	Log-transformed	0.0357	-0.1513	-0.9843	0.9	0.5	95% C.I.: 4.3 to 14.4%

Figures

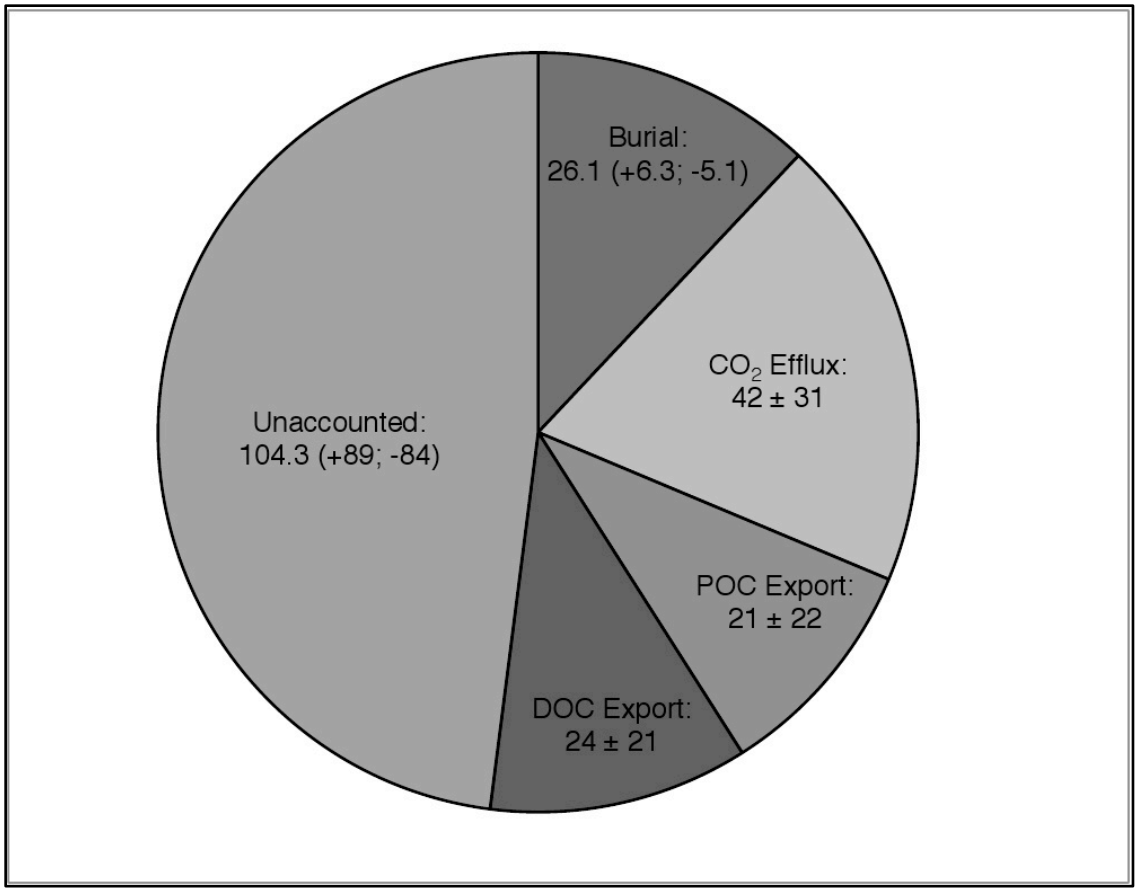

Figure 1. Fates of mangrove production (Tg C yr^{-1}). Revised from Bouillon et al. (2008).

List of References

Allen, S. E. (1974). Chemical analysis of ecological materials. New York: Wiley.

Alongi, D. M. (2009). The energetics of mangrove forests. S.l.: Springer.

Alongi, D., J. Pfitzner, L. Trott, F. Tirendi, P. Dixon, and D. Klumpp (2005), Rapid sediment accumulation and microbial mineralization in forests of the mangrove in the Jiulongjiang Estuary, China, *Estuarine, Coastal and Shelf Science*, *63*(4), 605-618, doi:10.1016/j.ecss.2005.01.004.

Alongi, D., A. Sasekumar, V. Chong, and J. Pfitzner (2004), Sediment accumulation and organic material flux in a managed mangrove ecosystem: estimates of land-ocean-atmosphere exchange in peninsular Malaysia, *Marine geology*, *208*(2-4), 383-402, doi:10.1016/j.margeo.2004.04.016.

Alongi, D., F. Tirendi, P. Dixon, and L. Trott (1999), Mineralization of organic matter in intertidal sediments of a tropical semi-enclosed delta, *Estuarine, Coastal and Shelf Science*, *48*(4), 451-467, doi:10.1006/ecss.1998.0465.

Alongi, D., G. Wattayakorn, J. Pfitzner, and F. Tirendi (2001), Organic carbon accumulation and metabolic pathways in sediments of mangrove forests in southern Thailand, *Marine Geology*, *179*(1-2), 85-103, doi:10.1016/S0025-3227(01)00195-5.

Barr, J. G., V. Engel, T. J. Smith, and J. D. Fuentes (2011), Hurricane disturbance and recovery of energy balance, CO2 fluxes and canopy structure in a mangrove forest of the Florida Everglades, Agricultural and Forest Meteorology, doi:10.1016/j.agrformet.2011.07.022.

Berner, R. A. (1982). Burial of Organic Carbon and Pyrite Sulfur in the Modern Ocean: Its Geochemical and Environmental Significance. American Journal of Science, 282, 451-473.

Bouillon, S. (2011), Carbon cycle: Storage beneath mangroves, *Nature Geoscience*, *4*(5), 282-283, doi:10.1038/ngeo1130.

Bouillon, S. et al. (2008), Mangrove production and carbon sinks: A revision of global budget estimates, *Global Biogeochemical Cycles*, *22*(2), 1-12, doi:10.1029/2007GB003052.

Brunskill, G. (2002), Carbon Burial Rates in Sediments and a Carbon Mass Balance for the Herbert River Region of the Great Barrier Reef Continental Shelf, North Queensland, Australia, *Estuarine, Coastal and Shelf Science*, *54*(4), 677-700, doi:10.1006/ecss.2001.0852.

Brunskill, G.J., Zagorskis, I. & Pfitzner, J. (1998), Carbon burial rates in sediments of the Herbert River region of the Great Barrier Reef continental shelf, North Queensland, Australia., in *CO2 Fixation and Storage in Coastal Ecosystems, Phase I Collected Reports (Ayukai, T., ed).*, pp. 1-20, Townsville.

Brunskill, G., I. Zagorskis, J. Pfitzner, and J. Ellison (2004), Sediment and trace element depositional history from the Ajkwa River estuarine mangroves of Irian Jaya (West Papua), Indonesia, *Continental Shelf Research*, *24*(19), 2535-2551, doi:10.1016/j.csr.2004.07.024.

Cahoon, D. R., and J. C. Lynch (1997), Vertical accretion and shallow subsidence in a mangrove forest of, *Mangroves and Salt Marshes*, *2100*, 173-186.

Callaway, J., R. DeLaune, and W. Patrick Jr (1997), Sediment accretion rates from four coastal wetlands along the Gulf of Mexico, *Journal of Coastal Research*, *13*(1), 181–191.

Cardona, P., and L. Botero (1998), Soil Characteristics and Vegetation Structure in a Heavily Deteriorated Mangrove Forest in the Caribbean Coast of Colombia, *Biotropica*, *30*(1), 24–34.

Chen, R., and R. R. Twilley (1999), A simulation model of organic matter and nutrient accumulation in mangrove wetland soils, *Biogeochemistry*, *44*(1), 93-118, doi:10.1007/BF00993000.

Chmura, G. L., S. C. Anisfeld, D. R. Cahoon, and J. C. Lynch (2003), Global carbon sequestration in tidal, saline wetland soils, *Global Biogeochemical Cycles*, *17*(4), doi:10.1029/2002GB001917.

Dittmar, T., N. Hertkorn, G. Kattner, and R. J. Lara (2006), Mangroves, a major source of dissolved organic carbon to the oceans, *Global Biogeochemical Cycles*, *20*(1), 1-7, doi:10.1029/2005GB002570.

Donato, D. C., J. B. Kauffman, D. Murdiyarso, S. Kurnianto, M. Stidham, and M. Kanninen (2011), Mangroves among the most carbon-rich forests in the tropics, *Nature Geoscience*, *4*(5), 293-297, doi:10.1038/ngeo1123.

Duarte, C. M., J. J. Middelburg, and N. Caraco (2005), Major role of marine vegetation on the oceanic carbon cycle, *Biogeosciences*, *2*(1), 1-8, doi:10.5194/bg-2-1-2005.

Duarte, C. M., and J. Cebrián (1996), The fate of marine autotrophic production, *Limnology and Oceanography*, *41*(8), 1758-1766, doi:10.4319/lo.1996.41.8.1758.

Eong, O. J. (1993), Mangroves-a carbon source and sink, *Chemosphere*, *27*(6), 1097–1107.

FAO, (2003), State of the World's Forests, 151pp., Food and Agriculture Organization of the United Nations, Rome.

Gilman, E., J. Ellison, and R. Coleman (2007), Assessment of mangrove response to projected relative sea-level rise and recent historical reconstruction of shoreline position., *Environmental monitoring and assessment*, *124*(1-3), 105-30, doi:10.1007/s10661-006-9212-y.

Gilman, E. L., J. Ellison, N. C. Duke, and C. Field (2008), Threats to mangroves from climate change and adaptation options: A review, *Aquatic Botany*, *89*(2), 237-250, doi:10.1016/j.aquabot.2007.12.009.

Gonneea, M. E., A. Paytan, and J. A. Herrera-Silveira (2004), Tracing organic matter sources and carbon burial in mangrove sediments over the past 160 years, *Estuarine, Coastal and Shelf Science*, *61*(2), 211–227, doi:10.1016/j.ecss.2004.04.015.

Harmon, T.S. (2011), Anthropogenic Changes Over the Last 100 Years in Dove Sound, Upper Florida Keys, USA. (Masters Thesis). Department of Environmental Science and Policy, University of South Florida, Saint Petersburg, FL, USA.

Hedges, J. I., and R. G. Keil (1995). Sedimentary organic matter preservation: an assessment and speculative synthesis, Mar. Chem., 49, 81–115.

Jennerjahn, T., and V. Ittekkot (2002), Relevance of mangroves for the production and deposition of organic matter along tropical continental margins, *Naturwissenschaften*, *89*(1), 23-30, doi:10.1007/s00114-001-0283-x.

Langley, J. A., K. L. McKee, D. R. Cahoon, J. a Cherry, and J. P. Megonigal (2009), Elevated CO2 stimulates marsh elevation gain, counterbalancing sea-level rise., Proceedings of the National Academy of Sciences of the United States of America, 106(15), 6182-6, doi:10.1073/pnas.0807695106.

Lynch, J. C. (1989), Sedimentation and nutrient accumulation in mangrove ecosystems of the Gulf of Mexico, University of Southwestern Louisiana, Lafayette, LA.

López-Medellín, X., E. Ezcurra, C. González-Abraham, J. Hak, L. S. Santiago, and J. O. Sickman (2011), Oceanographic anomalies and sea-level rise drive mangroves inland in the Pacific coast of Mexico, *Journal of Vegetation Science*, *22*(1), 143-151, doi:10.1111/j.1654-1103.2010.01232.x.

McKee, K. L., and J. E. Rooth (2008), Where temperate meets tropical: multi-factorial effects of elevated CO_2, nitrogen enrichment, and competition on a mangrove-salt marsh community, Global Change Biology, 14(5), 971-984, doi:10.1111/j.1365-2486.2008.01547.x.

Mcleod, E., G. L. Chmura, S. Bouillon, R. Salm, M. Björk, C. M. Duarte, C. E. Lovelock, W. H. Schlesinger, and B. R. Silliman (2011), A blueprint for blue carbon: toward an improved understanding of the role of vegetated coastal habitats in sequestering CO_2, *Frontiers in Ecology and the Environment*, 110621060659096, doi:10.1890/110004.

Ruiz-Fernández, A. C., J. L. Marrugo-Negrete, R. Paternina-Uribe, and L. H. Pérez-Bernal (2011), 210Pb-derived Sedimentation Rates and Corg Fluxes in Soledad Lagoon (Cispatá Lagoon System, NW Caribbean Coast of Colombia), *Estuaries and Coasts*, doi:10.1007/s12237-011-9394-6.

Sanders, C. J., I. R. Santos, E. V. Silva-Filho, and S. R. Patchineelam (2006), Mercury flux to estuarine sediments, derived from Pb-210 and Cs-137 geochronologies (Guaratuba Bay, Brazil)., *Marine pollution bulletin*, *52*(9), 1085-9, doi:10.1016/j.marpolbul.2006.06.004.

Sanders, C. J., J. M. Smoak, a. S. Naidu, D. R. Araripe, L. M. Sanders, and S. R. Patchineelam (2009), Mangrove forest sedimentation and its reference to sea level rise, Cananeia, Brazil, *Environmental Earth Sciences*, *60*(6), 1291-1301, doi:10.1007/s12665-009-0269-0.

Sanders, C. J., J. M. Smoak, a. S. Naidu, L. M. Sanders, and S. R. Patchineelam (2010), Organic carbon burial in a mangrove forest, margin and intertidal mud flat, *Estuarine, Coastal and Shelf Science*, *90*(3), 168-172, doi:10.1016/j.ecss.2010.08.013.

Sanders, C. J., J. M. Smoak, L. M. Sanders, a. Sathy Naidu, and S. R. Patchineelam (2010), Organic carbon accumulation in Brazilian mangal sediments, *Journal of South American Earth Sciences*, *30*(3-4), 189-192, doi:10.1016/j.jsames.2010.10.001.

Sanders, C. J., J. M. Smoak, L. M. Sanders, M. N. Waters, S. R. Patchineelam, and M. E. Ketterer (2009), Intertidal mangrove mudflat 240+239Pu signatures, confirming a 210Pb geochronology on the southeastern coast of Brazil, *Journal of Radioanalytical and Nuclear Chemistry*, *283*(3), 593-596, doi:10.1007/s10967-009-0418-7.

Scholl, D. W., F. C. S. Craighead, and M. Stuiver (1969), Florida Submergence Curve Revised : Its Relation to Coastal Sedimentation Rates, *Science*, *163*(3867), 562-564.

Tateda, Y., D. D. Nhan, G. Wattayakorn, and H. Toriumi (2005), Preliminary evaluation of organic carbon sedimentation rates in Asian mangrove coastal ecosystems estimated by 210Pb chronology, *Radioprotection*, *40*, 527-532, doi:10.1051/radiopro.

Twilley, R., R. Chen, and T. Hargis (1992), Carbon Sinks in Mangroves and their Implications to Carbon Budget of Tropical Coastal Ecosystems, *Water, Air, & Soil Pollution*, *64*(1), 265–288.

Woodroffe, C. (1981), Mangrove swamp stratigraphy and Holocene transgression, Grand Cayman Island, West Indies, *Marine Geology*, *41*(3-4), 271-294, doi:10.1016/0025-3227(81)90085-2.

Zimmerman, A., and E. A. Canuel (2000), A geochemical record of eutrophication and anoxia in Chesapeake Bay sediments: anthropogenic influence on organic matter composition, Marine Chemistry, 69(1-2), 117-137.

Chapter 2:

Blue Carbon in the Coastal Everglades: A Preliminary Measurement of Centennial-scale Burial Rates In Mangrove Soils

Introduction

The production, pathways and fates of organic carbon (OC) in mangrove systems have been discussed in a wide body of literature (Alongi et al., 1998; Bouillon et al., 2008b; Chmura, et al., 2003; Duarte et al., 2005; Duarte & Cebrián, 1996; Mcleod et al., 2011; Twilley et al., 1992). Although representing a relatively small percentage of the overall marine surface area, mangroves nonetheless are of great interest for the magnitude of their ecological and economic contributions, including their functioning in the global carbon cycle. Carbon in the form of inorganic CO_2 is assimilated from the atmosphere into the coastal zone through mangrove photosynthesis and the production of organic matter including leaves, woody material, and roots. As the plant material dies, detritus in the form of leaf litter, wood, bark, seeds and roots accumulate on or within the soil. Peat formation occurs where the organic material contributes a substantial percentage of the soil due to inundation with water in which the suboxic and anoxic conditions prevent decomposition.

Mangroves are estimated to bury 163 g OC m^{-2} yr^{-1} at the local scale, or 26.1 Tg yr^{-1} globally (Breithaupt et al., in Review), but there are numerous regional gaps in this estimate. This paucity of measurements provides reason for some uncertainty when

estimating the burial rate of carbon within systems that are governed by different control mechanisms. There are many factors that contribute to the preservation of soil OC including abiotic (e.g. topography, climate, mineralogy, frequency and extent of inundation) and biotic conditions including plant functional traits (e.g. above- and below-ground production inputs, turnover, and carbon allocation) and the influence of other biota on retention, consumption, or exposure to oxidation (e.g saprophytes and crabs) (Amundson, 2001; Davidson & Janssens, 2006; De Deyn et al., 2008; Kristensen, 2008; Smith et al., 1991). Additionally, the definition of the term "burial" (which may also be referred to as soil storage or accumulation) depends on the establishment of a timescale of interest. This is because organic material stored in the soil is subject to continual degradation and remineralization as well as biological and/ or physical mixing. On an annual scale, labile carbon near the soil surface, where tidal conditions are most conducive to oxidizing conditions, can be re-mineralized due to diagenetic processes that may remove 70-90% of the initial fraction on an annual basis (Duarte & Cebrián, 1996). An increasing number of studies have utilized ^{210}Pb as a tracer of the net OC accumulation rate in mangrove soils across a centennial time-span in order to assess the response of these systems to recent sea level rise as well as accounting for their capacity to sequester OC from the atmosphere on a scale of recent climate change (Alongi et al., 2004; Alongi et al., 2001; Brunskill, 2002; Sanders et al., 2012).

This research aims to provide a preliminary estimate for the centennial scale OC burial rate in the mangroves of the southwestern Everglades, near the mouth of the Shark River. Based on conditions of high productivity (Barr et al., 2010; Barr et al., 2011) and high soil OC% (Castañeda-Moya et al., 2011) our first hypothesis is that the mean burial

rate in this forest would exceed the global average. A secondary objective was to analyze the spatial variation in burial rates, testing the hypothesis that the landscape scale pattern of decreasing sedimentation and OC burial with distance from open water (Chen & Twilley, 1999; Furukawa & Wolanski, 1996) would be reflected at the site level, with burial rates being highest near the main creek of the Shark River and decreasing with distance toward the interior of the island. A tertiary objective was to examine the role of hurricane Wilma (2005) on the overall OC burial rate at this site. Based on results from two cores (SH3-1 at this site, and another from the Harney River ~7 km north of this site) (Smoak et al., in Review) our third hypothesis was that there would be a substantial increase in both mass and OC accumulation rates across the site in the Post-2000 time interval influenced by Wilma. Additionally, we investigated a hypothesis raised by Smoak et al. (in Review) that the elevated OC burial rate following Wilma was controlled by two different mechanisms: 1) increased production from storm delivery of P-rich sediment, and 2) storm surge redistribution of previously buried OC.

Methods

Study Site

The site for this study is an estuarine mangrove island approximately four km inland from the Gulf of Mexico on the Shark River in Everglades National Park (Figure 1). The mangrove species present are red (*Rhizophora mangle*), black (*Avicennia germinans*), and white (*Laguncularia racemosa*), with a canopy height of approximately 13 to 17 m (Whelan et al., 2009), stem densities ranging from 2,000-6,000 per hectare, and diameters at breast height ranging from 10-50 cm (Smoak et al., in Review). The

average soil surface is approximately 0.2 m above mean sea level and average pore water salinity is 24.6 ± 2.4 g l^{-1} (Krauss et al., 2006). Several elevation lows in the form of tidal rivulets within the forest were noted in the area where cores were taken. Local tides are semi-diurnal with an average amplitude ranging from 0.5 to 1.0 m, and much of the site is completely inundated twice a day (Barr et al., 2010; Romigh et al., 2006). The soil at the site is composed of 5.5 m of mangrove peat above the limestone bedrock (Whelan et al., 2005). This peat signature is indicative of a system whose soil accumulation is due primarily to autochthonous sources of mangrove litter (from roots to shoots) rather than deposition of terrigenous material from upstream runoff and erosion. The lack of substantial terrigenous input via the upstream freshwater flow is accompanied by a similar limitation in phosphorous, the primary limiting nutrient to macrophyte growth, including mangroves, in the Everglades (Childers et al., 2006; Noe et al., 2001). This upstream limitation is countered by provision of P from the Gulf of Mexico (Chen & Twilley, 1999; Fourqurean et al., 1992), leading to the description of the coastal Everglades as an "upside down estuary" (Childers et al., 2006) with the highest productivity found in the belt of mangroves along the southwestern extent where this research was conducted.

Included at this site as part of the AmeriFlux network (Baldocchi et al., 2001) is an eddy covariance flux tower with the capability of measuring exchange of carbon, water vapor and energy fluxes. Details of the tower's construction and instrumentation can be seen in Barr et al. (2010). The fetch boundaries for the flux tower encompass the entire island, and thus provide a site boundary for comparing soil OC accumulation with net ecosystem production (NEP) measurements. In 2004 & 2005 the measured NEP was

1,170 g OC m^{-2} yr^{-1} (Barr et al., 2010) and falls within the expected bounds of the most recent global estimate of mangrove Net Primary Production (NPP) of 1,363 ± 450 (down-scaled from the global 218 TG yr^{-1} in Bouillon et al., 2008b).

The region of South Florida where this site is located has been impacted by at least four major hurricanes since 1929 (Smith et al., 2009; 2010). In 2005 Hurricane Wilma passed just north of the site and left a strong signal of fine-grained carbonate marine sediment up to 56 mm thick near the river that decreased with distance inland (Whelan et al., 2009). This layer was shown to have a high concentration of phosphorous (Castañeda-Moya et al., 2009). Although previous storms have influenced this forest, the recent occurrence of hurricane Wilma provides a unique opportunity to examine the sedimentary signature at this site.

Soil Sampling & Processing

Seven 50-cm deep cores were retrieved utilizing a Russian peat corer at distances ranging from 25 to 170 m from the main creek of the Shark River (Figure 1; Table 1), all well within the footprint of the flux tower. The dimensions of a retrieved half core measure 5.0 cm in diameter by 50 cm long. The volume of a 1 cm interval is 9.82 cm^3. Sampling locations were chosen to obtain a representative spatial variance. Cores SH3-1, 3 and 7 were situated in a mix of black and white mangroves. Core SH3-5 was surrounded predominantly by black mangroves with a few white mangroves in proximity. Cores SH3-8 and 9 were retrieved within 1 m of each other, surrounded mostly by red mangroves. An additional core (SH3-4) was collected near core SH3-5. The high water content in the upper intervals of core SH3-4 limited the amount of material available for

dating, however some coarse woody material from this core was used for separate analyses of carbon content. SH3-1 was retrieved in February, and SH3-3 in December of 2009. The remaining five cores were taken in November of 2010. Cores were enclosed in airtight plastic sleeves and transported in a cooler to the laboratory for refrigeration prior to processing.

Each core was sectioned in 1 cm intervals, with the exception of SH3-1, which was sectioned in 2 cm intervals beginning at 10 cms depth. An aliquot was taken from each interval for gravimetric analyses of wet weight, dry weight, and loss-on-ignition weight (LOI). Dry weight was obtained by drying at 105°C for 24 hours, and LOI was obtained by heating in a furnace at 550°C for one hour. For SH3-1 the aliquot volume was 4.17 cm^3. For the other 5 cores the aliquot volume was 1.131cm^3. Aliquots were intended to be representative of each interval's soil composition, however some sampling bias was functionally necessary to exclude coarse woody material whose retrieval would have disturbed the aliquot volume. In the uppermost layers in which there was a clear visible distinction between the dark brown peat and the gray carbonate material delivered by hurricane Wilma, the aliquot was sampled in order to proportionally represent both.

Coarse woody material in the intervals merited separate attention because of its occasional exclusion from aliquot sub-sampling. In this peaty soil the coarse material consists of a continuum of material ranging from roots (≥ 1mm diameter), twigs, bark, and leaves (Figure 2). Following freeze-drying, this coarse material was separated during the process of homogenizing each interval's sediments. The criteria for separation were that the material's size and tenacity would disrupt the collection of the aliquot volume. Following freeze-drying, coarse material was removed from individual intervals in cores

SH3-7 & 8 and placed in pre-weighed crucibles for gravimetric analyses of dry weight and LOI. Coarse material was analyzed en masse rather than by interval for cores SH3-3, 9, & 4; the material was homogenized then separated for gravimetric analyses and OC measurement. Note that SH3-4 was not a dated core, but the coarse material was separated and analyzed to the same dateable depths as the other cores. There was no coarse woody material found in SH3-5, and SH3-1 was processed before the decision was made to examine this material.

The OC from this coarse material was added into calculations to consider whether it might alter the OC accumulation rates based only on the aliquot material. Total mass for each sectioned interval of the core was first calculated by multiplying the original aliquot dry-bulk-density by the total volume (9.8175 cm^3). The weighed coarse material mass was then substituted into the calculated mass, providing an interval estimate of total fine and coarse OC (measured in grams per interval). The area of a core interval then was scaled up to the square meter scale for comparison with measurements based only on aliquots. Note that this examination of individual intervals was only conducted for Cores SH3-7 & 8 for reasons cited in the previous paragraph.

Core Dating & Rate Calculation

Soil accumulation rates were determined using ^{210}Pb, a radionuclide with a half-life of 22.3 years. Before being deposited to the land surface, ^{210}Pb is found in the atmosphere where it has evolved from ^{226}Ra ($t_{1/2}$ = 1,600 years) which subsequently decays to ^{222}Rn ($t_{1/2}$ = 3.8 days) and escapes from the crust of the lithosphere. The ^{210}Pb is deposited via atmospheric fallout on plants, soil or water where its particle-reactive

nature results in adsorption, primarily to clays and organic compounds. As a result, when organic matter accumulates in peaty soils such as those found beneath mangroves in the southwestern Everglades, the ^{210}Pb accumulates over time and its half-life can be used to determine the age of the soil.

The sectioned intervals (minus aliquots) were placed in labeled plastic tubs and freeze-dried in preparation for dating. The soil was subsequently homogenized using a mortar and pestle, then packed in pre-weighed gamma counting tubes and reweighed. Each tube was sealed and set aside for three weeks to create secular equilibrium between ^{226}Ra and ^{214}Pb. Lead-210 and ^{226}Ra were measured using an intrinsic germanium well detector coupled to a multi-channel analyzer. Activities were calculated by multiplying the counts per minute by a factor that includes the gamma-ray intensity and detector efficiency determined from standard calibrations. Lead-210 activity was determined using the 46.5 KeV gamma peak and ^{226}Ra activity was determined using the 351.9 KeV peak. Sections were counted down the depth of the core until the calculated value of the ^{226}Ra activity equaled the ^{210}Pb activity; at this depth it is no longer possible to distinguish the unsupported ^{210}Pb from that supported by the in situ decay of ^{226}Ra. Additionally, because the dating models utilize the activity of ^{210}Pb per unit of material mass, this coarse woody material previously referred to, is commonly removed to provide the most accurate model-derived date for the soil. To confirm this, five samples of coarse woody material were measured for gamma ray activity, and ^{210}Pb was below detection limits for each one. This conclusion is supported by studies that have specifically examined the uptake of ^{210}Pb by plant roots in controlled experiments (Hovmand et al., 2009).

The sampling site in southwest Florida is subject to hurricane activity, and the storm surge that accompanies such events can be a source of significant marine sediment deposition (Castañeda-Moya et al., 2009; Whelan et al., 2009; Smith et al., 2009). Because of this, the soil accumulation rate has been calculated following the Constant Rate of Supply (CRS) model. This model is intended for use in systems in which the initial concentration of unsupported ^{210}Pb is periodically diluted by an increase in local production or an addition of allochthonous material (Appleby & Oldfield, 1978). Dates derived for the bottom of each interval enabled the calculation of four rates used in this study:

1. Mass Accumulation Rate = interval mass (mg cm^{-2}) / # of years in interval
2. Soil Accretion Rate = interval depth (mm) / # of years in interval
3. OC Burial Rate = (OC% in interval × interval mass (mg cm^{-2})) / # of years in interval
4. Inorganic Matter Accumulation Rate = (interval mass – organic matter mass) / # of years in the interval.

In general, the interest of this paper is to examine the century-scale rates. However, the CRS model also attributes dates to each soil interval and provides the opportunity to examine decadal variability in the rates. In examining the temporal variability of the entire site with a decadal resolution, an average of the rates for all six cores needs to be standardized to common intervals. This requires some adjustments because the model dates at the bottom of each soil interval do not correspond from one core to the next due to different accumulation rates. The depths need to be re-segmented by age rather than depth. The decade break was used as a fraction of the number of years in the interval

(Figure 3). This age fraction was then applied to the mass and subsequently divided by the number of years in the age interval to determine the accumulation rate. This method assumes a constant rate of accumulation within the given interval, which is problematic in consideration of pulse events, but unlikely to misconstrue long-term trends.

C:N & Stable Isotopes ($\delta^{13}C$ & $\delta^{15}N$)

Soil from intervals in SH3-1 and 9 were acidified to remove carbonate material prior to analysis of C, N, $\delta^{13}C$, and $\delta^{15}N$. These two cores were selected as representative samples for the site as they are from the forest nearest the river and furthest inland. Samples were processed by the University of California Davis Stable Isotope Facility using a PDZ Europa ANCA-GSL elemental analyzer connected to a PDZ Europa 20-20 isotope ratio mass spectrometer. Coarse root material from cores SH3-3, 9, & 4 was analyzed for OC% at the Florida International University Southeast Environmental Research Center Lab using a Finnigan Delta C EA-IRMS (with TC/EA).

Results

Results and profiles of gravimetric analyses for dated intervals from each core are presented in Table 2 and Figure 4. The mean dry bulk density (DBD) for all dated intervals (n=108) is 0.21 ± 0.10 g cm^{-3} with the highest DBD near the river (0.28 ± 0.18 g cm^{-3}), and the lowest furthest inland(0.16 ± 0.03 g cm^{-3}). The mean OM percentage is 52 ± 13, with the lowest percentage in the two cores nearest the river, increasing at the four inland cores.

Organic Carbon was measured for homogenized bulk sediments in two cores (all intervals in SH3-1; 12 of 25 intervals in SH3-9; total n=39). Measured organic carbon percentages for cores SH3-1 and SH3-9 were 19 ± 6% and 25 ± 4% respectively (Table 2). Results for OC% and OM% (via LOI) of these two cores were subjected to linear regression analysis to determine a conversion calculation for the OC% in cores that were not instrumentally analyzed. Equation 1 produced by the regression line for bulk sediments ($R^2 = 0.844$) is:

$$OC\% = (0.4263 \times OM) + 0.0097 \quad (1)$$

This high R^2 is influenced by three OM values lower than 15%. The mean of the OC/OM fraction for all intervals is 45 ± 6, and the mean of the fraction for the three low-OM values is 50 ± 11. Consequently Equation 1 is expected to be a slightly conservative estimate of OC as a percentage of OM. Using Equation 1 to calculate the OC% of the remaining cores, the site average is 23 ± 5%. Stable isotope values were the same for both measured cores with an average of -27.56 for $\delta^{13}C$ and 3.25 for $\delta^{15}N$. The C/N ratio for core SH3-1 was 19.78, slightly lower than the value of 22.36 for core SH3-9 (Table 5).

Each of the six cores shows a net decrease in the activity of excess ^{210}Pb (Table 2). Each also exhibits lower activity in the near-surface intervals that corresponds to dilution from hurricane Wilma's input of marine carbonate sediment that is low in ^{210}Pb. Although often used to corroborate ^{210}Pb dates, there was no distinct ^{137}Cs peak visible in these cores due to its mobility in these highly organic soils that lack clays. This lack of independent confirmation of the dates does add to the uncertainty of the model-calculated ages. Additionally, while there is a net decrease with depth, there are several un-

characteristic peaks in the excess ^{210}Pb below 20 cm depth that may correspond to advective mixing from crab burrows. However, the CRS dating model is relatively insensitive to mixing (Appleby & Oldfield, 1992) and although the date specified to the particular *soil* might be inaccurate, it is not expected to negatively impact the estimate of the date for that *depth* in relation to the intervals above and below it.

The overall mass accumulation rate for the site is 600 ± 153 g m^{-2} yr^{-1} (95% C.I.), ranging from 429 at SH3-9 to 903 at SH3-1. The combined decadal intervals display a trend of steady increase, ranging from 205 in the earliest, deepest intervals to 1,491 g m^{-2} yr^{-1} in the surface intervals. The 95% confidence interval for the mean OC burial rate from all six cores at this site is 124 ± 32 g m^{-2} yr^{-1}. The OC accumulation rates show a slight spatial variation for the six cores, however there is no linearity in terms of distance from open water ($R^2 = 0.04$). The rates for the six cores are 151, 90, 133, 112, 151, & 106 g OC m^{-2} yr^{-1} over a distance of 170 m from the main channels of the Shark River (Figure 1). Of particular interest is the difference in rates between cores 8 and 9, that are only 1 m apart. SH3-1 and SH3-8 share the greatest overall rate despite their respective locations being 25 and 150 m inland. SH3-3 is the second nearest the water (35m inland) and has the lowest OC burial rate. Temporally, the site mean burial rate has increased from 40 g OC m^{-2} yr^{-1} in the first decade of the 20th century, to 212 at the surface for the years 2000-2010.

The OC content of the coarse material from cores SH3-3, 9, & 4 was determined to be 45 ± 3% of the OM. Equation 2 was used to determine the OC% from the OM measurements from cores SH3-7 & 8:

$$OC\% = (0.45 \times OM) \quad (2).$$

The estimated coarse OC was substituted into the OC accumulation rates to determine its impact (Table 4). Several interval depths showed a marked increase in OC accumulation due to the presence of coarse root material. The 1933-1939 interval is one notable example from SH3-7 that increased by almost 18 g OC m^{-2} yr^{-1}. In Core SH3-8 notable increases are seen in intervals 2004-2006 and 1995-1997 with respective increases of 9.8 and 6.1 g OC m^{-2} yr^{-1}. Overall, the exclusion of some of the coarse woody material from the aliquot sampling has no noticeable impact on the OC accumulation rates for the total measured periods. For SH3-7, inclusion of the coarse OC only adds to the annual accumulation rate by 1.62 g OC m^{-2} yr^{-1}; for core SH3-8 the inclusion only adds 2.7 g OC m^{-2} yr^{-1}.

The soil depth/ time provides the rate at which the surface has accreted over the dated time frame. Surface accretion corresponds to increased mass at the surface, which has a compacting effect on the underlying layers. Therefore the interval depths of lower bulk density have been normalized to the density of the bottom layers (Lynch et al., 1989). Several near-surface intervals with higher DBD in the Wilma layer were not adjusted. The density-corrected mean accretion rate from all six cores is 2.8 ± 0.40 mm yr^{-1} (95% C.I.), and ranges from 2.3 at SH3-3 and SH3-7 to 3.6 at SH3-1 nearest the river. Over the past century, the density corrected accretion rates have increased from 1.0 mm yr^{-1} from 1900-1910 to 4.8 from 2000-1010.

Discussion

Site Carbon Accumulation Rate

Contrary to the expectations of our first hypothesis, the mean OC burial rate in the coastal Everglades (124 g OC m^{-2} yr^{-1}) is not greater than the global average of 163 g OC m^{-2} yr^{-1} (Breithaupt et al., in review). The 95% confidence interval for the difference of the two mean burial rates is from 2 – 76 g OC m^{-2} yr^{-1}. This is somewhat unexpected given the combination of high productivity (Barr et al., 2010) and high sedimentary OC% (Figure 4; Castañeda-Moya et al., 2011). This mean rate is slightly greater than the rate of 86 g OC m^{-2} yr^{-1} found 96 km northwest of the site in Rookery Bay, FL (Lynch, 1989), and is slightly less than a rate of 147 g OC m^{-2} yr^{-1} in the Florida Keys (Callaway et al., 1997). The site mean OC% of 22.7 ± 4.7% for 108 dated soil intervals is substantially higher than the global median of 2.2% (Kristensen et al., 2008). These findings indicate that something more than NEP and soil OC% is needed to qualitatively predict the local OC burial rate in comparison to the global average.

The characterization of mangrove geomorphic settings has been broadly delineated between oceanic/fringe and estuarine/ riverine-delta to potentially account for differences in the provision of autochthonous and allochthonous sources of sediment and/or litter (Donato et al., 2011). Although this site is generally categorized as a riverine mangrove forest, for the purposes of comparison according to sedimentary provision, it would be more appropriate to classify this system as fringing/oceanic. This is supported by two arguments. First, the Everglades in general, and the Shark River specifically, deliver very little terrigenous mineral sediments. Second, the soil OC% of oceanic and riverine settings in the Indo-Pacific is 14.6 and 7.9 respectively (Donato et al, 2011). The

soil OC% of this site in the Everglades is 23%, greater than that of the high organic oceanic mangroves. In terms of the OC density, the mean for this site (0.048 g cm^{-3}) is greater than the mean for oceanic (0.038 g cm^{-3}) and less than that of riverine (0.061 g cm^{-3}) (Donato et al., 2011). The indication is that these mangroves are largely dependent on their own production for sustaining their soil growth and support of the forest substrate. Next, it is useful to examine both the spatial and temporal variability in the rates at this site to provide a more complete answer for why the Everglades burial rate is lower than the global rate.

Spatial Variability of Accumulation Rates

Model expectations indicate that burial rates on a large scale will be greatest near open water, the location of allochthonous delivery, and recede with distance into the forest; similarly expectations indicate high bulk density near the water, and higher OM% further inland (Chen & Twilley, 1999). The bulk densities and OM% at this site support the latter prediction. Additionally, our measurements for mean bulk density (0.21 ± 0.10 g cm^{-3}) and OC% (23 ± 5%) are virtually identical to former measurements taken at this site of 0.21 g cm^{-3} and 22.2 ± 1.2% providing some confirmation of steady site conditions in the past 15 years (Chen & Twilley, 1999). Regarding the former model prediction of *rates*, the trend has been confirmed on a smaller scale in a number of locations. OC burial rates taken from cores that were 20 m apart in a mangrove fringe and interior forest were 949 and 353 g m^{-2} yr^{-1} in Tamandare, Brazil, and were 234 and 192 g m^{-2} yr^{-1} in two cores taken 10 m apart in Cananéia, Brazil (Sanders et al., 2010). At two sites in Terminos Lagoon, Mexico burial rates declined with distance, from 185 to 61 g OC m^{-2}

yr^{-1} from two cores that were 85 m apart, and 122 and 59 from another two cores that were 215 m apart (Lynch, 1989). However in Rookery Bay, Florida there was no strong linear decline in OC burial rates, with rates from fringe to interior over a distance of 70 meters being 90, 69, 86, and 99 g OC m^{-2} yr^{-1} (Lynch, 1989). In contrast to our second hypothesis, a similar lack of correlation with distance ($r = 0.2$) is evidenced at this site in the coastal Everglades. These differences imply that there are numerous small-scale influences on local sedimentation and soil building including topography, small tidal rivulets, species root type (i.e. cable with pneumatophores or prop roots), and fine root production variability.

Although lacking a pattern of OC burial, the accumulation of inorganic matter does exhibit a pattern of decrease in sedimentation with distance inland ($r = 0.74$) in accordance with general sedimentation expectations (e.g. Furukawa & Wolanski, 1996). This pattern is even more noticeable ($r = 0.79$) if the accumulation of the most recent decade, including hurricane Wilma, is excluded. This single event added an enormous pulse of inorganic matter that is noticeable in the record from each core (Figure 5C), to the extent that some of the interior sites (Sh3-7 & 8) increased more than their pre-2000 patterns might predict. On the other hand, the correlation of diminishing OC burial rate with distance inland prior to the last decade disintegrates completely ($r = 0.06$), with the highest overall burial rate being found at core 8 (143 g OC m^{-2} yr^{-1}) 170 m into the forest, and the lowest rate at core 3 (83 g OC m^{-2} yr^{-1}) only 35 m into the forest. In this case, the Wilma pulse served to increase OC burial much more than predicted at SH3-7, largely erasing even the meager differences in OC burial rates from the prior century. The strong difference in the predictability of the accumulation rate as a function of distance for OC

and IM is evidence of different controlling mechanisms. The IM accumulation rate depends on hydrologic delivery, and OC accumulation responds to numerous factors including allochthonous hydrologic delivery, topographic variations, the presence of small tidal rivulets in the forest, reworking by benthic fauna, the favorability of oxidizing conditions (i.e. extent and duration of inundation), and above and belowground production variability. Our results indicate that landscape-scale predictions of OC burial rates are not consistent on a smaller site scale, providing some uncertainty for future sampling that endeavors to select a location representative of local OC burial rates.

The Influence of Hurricane Wilma

As anticipated by our third hypothesis, the influence of hurricane Wilma (2005) is noticeable throughout the Post-2000 interval (Table 3, Figures 5 & 6), with substantial increases in all 4 measured parameters. This evidence indicates that a hurricane pulse can momentarily transform this site from an oceanic system to one of riverine characteristics in which autochthonous soil production is supplemented in a major way by allochthonous marine sediments. This transformation is similar to the description of the coastal Everglades as an upside down estuary (Childers et al., 2006), but the emphasis is on the infrequent, significant delivery of sediments as much as the limiting nutrients.

The specific mechanism for the increased accumulation of OC in the soil has yet to be fully explained. One hypothesis (Smoak et al., in Review) is that a combination of two processes occur depending on proximity to open water, and whether the location is subject to storm surge scouring, storm surge deposition of transported previously buried organic matter, or storm surge deposition of P-rich marine marl (Castañeda-Moya et al.,

2009). In the case of the latter occurring, there follows the stimulation of additional biomass production. The rate of OC accumulation declines with depth in each of the six cores as exemplified in Figure 4B, and one question that might be raised by this profile is whether the OC accumulation rate has truly increased in the Wilma-influenced layer, or whether this increase in the past decade can simply be attributed to a greater concentration of surficial labile carbon that will ultimately degrade with time (i.e. depth). One method for addressing this is to look at the history of IM accumulation rates, which should not exhibit the same declining profile as OC over time, if degradation is the primary control (Figure 6C, Table 3). The IM accumulation rates from 2000-2010 are significantly higher than demonstrated in any previous decade of the past century and seem to indicate that hurricane Wilma contributed a unique accumulation influence on the site. This surface spike in IM correlates with the surface spike in OC, and the lower accumulation rates in the underlying layers look similar as well. If the IM declines with depth our supposition is that its supply was lower in those intervals. This assumption may follow for OC as well, since the OC accumulation rate also declines with depth. A hypothesis for future investigation is that an elevated OC accumulation rate in the Wilma decade will remain visible in the profile in future decades, even given the fact that the OC will continue to degrade in that time.

The Wilma record implies considerable importance to the role of hurricanes supporting this site in relation to sea level rise even though the signatures of previous storms have been diluted in the soil profiles. The mean density-corrected soil accretion rate over the past century is 2.8 ± 0.4 (95% C.I.) mm yr^{-1}. This is less than the accretion rate of 3.85 mm yr^{-1} measured from unpublished ^{137}Cs data cited by Castañeda-Moya et

al. (2009). Both of these rates are substantially lower than rates measured at this site in the 1990s of 8.9mm yr^{-1} (Chen & Twilley, 1999). Lower accretion rates of 1.6 mm yr^{-1} have been measured in Rookery Bay (Lynch et al., 1989). The lower rates in Rookery Bay are not unexpected as that site is not subject to the same open water influences as the Shark River. Our findings indicate that the forest floor at this site has essentially matched sea level rise of 2.24 ± 0.16 mm yr^{-1} over the past century as recorded at Key West (NOAA National Ocean Service). The overall accretion rate indicates the vital importance of the autochthonous contribution of OC to the soil. Without the 23% of the soil mass that is OC, the forest floor would be considerably lower than its present position and would consequently endure more stress from sea level rise. As it is, this OC does not contribute uniformly to the surface accretion, but is able to shrink and swell in response to various hydrologic conditions (Whelan et al., 2005). Finally, if the Wilma influence is subtracted the local accretion rate continues to match sea level, but falls to 2.6 mm yr^{-1}. This evidence of a beneficial hurricane impact from storm surge sediment deposition needs to be balanced with assessments of the destructive elements such as defoliation and tree loss, to consider net harm or benefit to the forest.

OC Accumulation and Net Ecosystem Production

Net ecosystem production was measured as 1170 g C m^{-2} yr^{-1} by the eddy flux tower at this site in 2004 and 2005 prior to the occurrence of hurricane Wilma (Barr et al., 2010). The 95% confidence interval for the mean pre-2000 burial rate is 95 to 133 g OC m^{-2} yr^{-1} (Table 3). This equates to between 7.9 and 13.3% of annual NEP. Overall, this is very similar to the global estimates of 8.1% (Bouillon et al. 2008b) and 11.4%

(Breithaupt et al., in Review). This local burial percentage assumes that 100% of burial is attributed to local mangrove production. This may not be the case due to general tidal and riverine import combined with storm surge events that have the potential to redistribute allochthonous OC not accounted for in local NEP. Development of additional research methods are necessary to differentiate how much soil OC is produced locally, and how much may be due to other origins, including that from mangrove forest further up- or downstream on the Shark River. Overall stable isotopes and ratios of C:N indicate only that the soil carbon is derived largely from mangrove organic matter (Table 5) (Bouillon et al., 2008a; Kristensen et al., 2008).

Additional Research Questions

As research into the pools and fluxes of C in mangrove environments continues to grow more refined and specific, it is increasingly necessary that the units of measurement be as specific as possible. For example, production is usually measured on an annual basis and is a long-running average that includes diurnal and seasonal variability, with resolution that often can document fractions of a minute. However, soil accumulation of OC is measured on many timescales with varying levels of resolution that range from days to decades. Usually the interest in a system's C cycle is related to climate feedbacks, and fluxes that operate on relatively long-term centennial timescales. For this reason ^{210}Pb can be a valuable tool for measuring OC burial. However, as evidenced at this site, ^{210}Pb reaches its maximum timescale at a relatively shallow depth (i.e. < 50 cm), which coincides with the zone of root production. To the best of our knowledge, none of the current estimates of OC burial rates have differentiated between the burial rate of

presumably dead OC and the accumulation of belowground biomass (Chmura et al., 2003; Breithaupt et al., in Review).

Very recently research at this site in the Everglades utilized in-growth measurements of belowground production over 1 and 3-year periods to document a site mean total root production rate in the shallow zone (< 45 cm) of ~ 370 g m^{-2} yr^{-1} and a fine-root production rate of ~150 g m^{-2} yr^{-1} (Castañeda-Moya et al., 2011). Fine roots are defined as having a diameter of < 2mm and made up the dominant fraction of our cores, though a few notable exceptions were found (Figure 2). The average LOI of our coarse woody material (which included things other than roots such as leaves, twigs, & bark) was 75%. And the average OC% of the coarse material was 33%. Applying these percentages, we can roughly estimate that these root production measurements represent 115 and 50 g OC m^{-2} yr^{-1} for total roots and fine roots respectively. The total root production is almost identical to our estimate of OC accumulation of 124 g m^{-2} yr^{-1} and raises important questions about the nature of what this research is actually measuring. The root production measurements were taken in early 2006 and therefore may include some additional biomass stimulated by the P-input in the Wilma marl, but this is unlikely to significantly alter the estimate (Whelan et al., 2009). Here again we need to be reminded of the timescales being used. Root biomass turnover varies based on size, and is estimated to range from 18 months for fine roots and up to 10 years for coarse roots (Castañeda-Moya et al., 2011). Therefore we can expect the loss of some of this OC to remineralization and export as dissolved OC via tidal pumping. Even so, these numbers offer substantial evidence that root production contributes a majority of the soil,

combined with litter and allochthonous import of inorganic matter such as that seen in the Wilma layer.

Conclusion

The southwestern coastal Everglades bury OC more slowly than the global average in spite of having high production rates and a high percentage of organic carbon in the soil. The ability of these mangroves to contribute to soil building and thus enable the forest floor to keep up with rising sea level is of critical importance because there is essentially no regular input of terrigenous sediment from up-stream. However, the autochthonous contribution to soil accumulation through OC production is supplemented by allochthonous material such as that exhibited following hurricane Wilma. Although Wilma caused considerable damage to the forest as a whole, results here demonstrate that this was offset to some extent by the beneficial influence of enhanced accretion as well as OC accumulation. The contributions of small-scale influences on soil building are noticeable at this site, revealed by different patterns in the organic and inorganic matter inputs. Examination of local belowground production rates further demonstrates the considerable importance of roots in the soil building process.

Great global attention has been given to the endangerment of these coastal wetland forests, and they have been positioned as vital interests in terms of preservation and conservation for their ecosystem services (Alongi, 2011). While deforestation from direct anthropogenic causes is of little concern in the Everglades today, the potential losses associated with rising sea level coupled to the destructive forces of blow-down and storm surge raise questions about the future of these mangroves in the southwest

Everglades. Although this site gives evidence of keeping pace with sea level rise, research of this nature is needed on a much wider scale to assess the net accretion and OC accumulation rate across the greater coastal Everglades. As has been shown in estuaries in China and Malaysia, single site assessments showing accretion and accumulation may not accurately account for cumulative losses occurring elsewhere in the system (Alongi, 2011). The implication may be that the addition of material at this site occurs at the expense of other locations in the Everglades. Add to this the uncertainty regarding the impacts of restoration of upstream freshwater flows and there is a need for research in the mangrove forests as well as the upstream marshes and downstream mudflats, to quantify both the stock of carbon presently buried in the soils as well as the century-scale burial rates.

Tables

Table 5. Core Collection Dates, Mangroves Species Present, & Distance from River.

Core ID	Collection Date	Mangrove Species Present	Distance from River (m)
SH3-1	February, 2009	Equal mix of Red and Black mangroves.	25
SH3-3	December, 2009	Equal mix of Red and Black mangroves.	35
SH3-4	November, 2010	Black mangroves predominate with a few White mangroves.	70
SH3-5	November, 2010	Black mangroves predominate with a few White mangroves.	50
SH3-7	November, 2010	Equal mix of Red and Black mangroves.	145
SH3-8	November, 2010	Dominated by Red mangrove prop roots.	170
SH3-9	November, 2010	Dominated by Red mangrove prop roots.	171

Table 6. Excess Pb-210 Activity, Model Age at Bottom of Each Interval, Dry Bulk Density, Organic Matter, & Organic Carbon Percentage by Depth Interval

	SH3-1[1]					SH3-3					SH3-5					SH3-7					SH3-8					SH3-9				
Depth Interval	$^{210}Pb_{XS}$ (dpm g^{-1})	Age	DBD (g cm^{-3})	OM%	OC%[2]	$^{210}Pb_{XS}$ (dpm g^{-1})	Age	DBD (g cm^{-3})	OM%	OC%[3]	$^{210}Pb_{XS}$ (dpm g^{-1})	Age	DBD (g cm^{-3})	OM%	OC%[3]	$^{210}Pb_{XS}$ (dpm g^{-1})	Age	DBD (g cm^{-3})	OM%	OC%[3]	$^{210}Pb_{XS}$ (dpm g^{-1})	Age	DBD (g cm^{-3})	OM%	OC%[3]	$^{210}Pb_{XS}$ (dpm g^{-1})	Age	DBD (g cm^{-3})	OM%	OC%[4]
0-1	1.9	2.6	0.88	13%	8%	3.7	1.5	0.23	30%	14%	4.7	1.0	0.17	61%	27%	4.4	2.8	0.41	27%	13%	4.1	2.0	0.34	35%	16%	4.4	2.1	0.26	26%	13%
1-2	1.0	3.5	0.54	12%	6%	4.4	4.3	0.35	29%	13%	5.0	2.2	0.17	61%	27%	4.1	5.3	0.37	29%	13%	3.8	4.1	0.35	34%	15%	4.3	3.7	0.20	39%	16%
2-3	1.0	4.6	0.69	11%	4%	3.9	6.9	0.32	30%	14%	5.2	3.4	0.17	60%	26%	4.3	7.4	0.27	38%	17%	3.9	6.4	0.35	32%	15%	7.6	5.9	0.14	55%	24%
3-4	4.4	6.2	0.21	42%	27%	4.4	9.7	0.28	32%	15%	4.2	5.9	0.43	20%	9%	4.7	9.8	0.27	41%	18%	4.3	10.2	0.48	24%	11%	7.4	8.1	0.14	60%	24%
4-5	6.2	8.4	0.19	48%	19%	3.6	12.0	0.28	33%	15%	4.4	7.3	0.20	54%	24%	4.9	14.8	0.47	28%	13%	4.4	13.4	0.36	30%	14%	6.8	10.4	0.14	50%	22%
5-6	5.7	10.3	0.16	53%	23%	3.9	13.8	0.18	43%	19%	7.1	9.4	0.18	50%	22%	4.3	18.5	0.36	33%	15%	4.1	15.1	0.19	52%	23%	7.2	13.0	0.15	63%	28%
6-7	6.6	12.7	0.17	52%	24%	5.6	16.1	0.15	45%	20%	5.4	11.1	0.19	60%	27%	4.2	23.3	0.41	27%	13%	6.1	17.4	0.16	63%	28%	7.3	16.1	0.16	56%	26%
7-8	4.4	14.6	0.19	54%	25%	4.7	18.2	0.16	45%	20%	5.1	12.6	0.15	66%	29%	4.4	26.2	0.21	51%	23%	5.5	20.1	0.19	65%	29%	7.0	18.3	0.11	61%	27%
8-9	5.3	16.9	0.17	52%	22%	4.4	21.1	0.21	40%	18%	5.3	14.3	0.18	57%	25%	4.9	30.6	0.26	49%	22%	4.2	22.1	0.17	64%	28%	6.3	21.4	0.15	63%	28%
9-10	3.4	18.3	0.17	44%	21%	4.4	23.7	0.18	47%	21%	5.0	15.9	0.16	61%	27%	4.8	34.2	0.18	56%	25%	3.8	24.1	0.18	60%	27%	5.3	24.1	0.14	61%	28%
10-11	4.5	22.2	0.21	49%	21%	3.1	25.3	0.15	49%	22%	5.6	18.4	0.21	51%	23%	4.3	38.1	0.20	60%	27%	3.7	26.2	0.18	67%	29%	4.2	26.8	0.17	62%	29%
11-12						3.4	28.1	0.21	45%	20%	5.4	20.3	0.16	57%	25%	5.5	42.3	0.15	61%	27%	4.4	28.3	0.14	68%	30%	3.3	28.3	0.11	62%	28%
12-13	2.9	24.9	0.21	45%	20%	3.7	31.1	0.19	38%	17%	4.1	22.3	0.20	56%	25%	5.0	47.6	0.18	69%	31%	4.3	31.1	0.18	59%	26%	3.5	30.9	0.17	56%	29%
13-14						3.6	33.8	0.16	50%	22%	4.2	24.2	0.17	66%	29%	2.9	49.9	0.12	65%	29%	3.7	34.1	0.21	64%	28%	2.7	33.2	0.18	57%	25%
14-15	2.8	28.0	0.22	44%	17%	3.5	36.6	0.15	46%	21%	4.5	25.7	0.12	68%	30%	3.0	52.4	0.11	65%	29%	3.4	37.0	0.20	55%	25%	3.0	36.1	0.19	56%	25%
15-16						3.3	39.6	0.17	50%	22%	4.3	27.1	0.12	67%	29%	3.0	56.7	0.18	61%	27%	3.3	39.8	0.18	62%	28%	3.0	38.1	0.12	65%	28%
16-17	2.6	33.1	0.22	46%	17%	3.1	43.1	0.18	47%	21%	4.4	29.1	0.15	64%	28%	3.6	61.9	0.16	61%	27%	3.2	42.4	0.16	62%	27%	3.2	40.7	0.13	56%	27%
17-18						3.0	47.5	0.21	42%	19%	4.9	31.5	0.15	65%	29%	2.7	66.9	0.17	60%	26%	3.1	44.8	0.14	61%	27%	3.3	43.6	0.13	62%	27%
18-19	2.0	36.2	0.25	48%	21%	2.5	51.5	0.20	40%	18%	4.7	33.4	0.12	65%	29%	2.2	71.9	0.18	58%	26%	2.9	47.5	0.16	60%	26%	3.8	49.4	0.21	58%	28%
19-20						2.4	55.9	0.20	39%	17%	4.5	36.0	0.16	64%	28%	2.1	77.8	0.19	58%	26%	2.7	50.5	0.17	60%	26%	3.8	55.3	0.17	56%	25%
20-21	2.6	40.8	0.27	40%	20%	2.5	61.8	0.23	39%	18%	5.1	39.0	0.14	64%	28%	1.8	83.2	0.16	59%	26%	2.9	54.6	0.20	59%	26%	3.7	61.0	0.14	54%	24%
21-22						2.3	67.6	0.20	41%	19%	5.3	42.7	0.15	61%	27%	1.9	89.5	0.15	60%	26%	2.6	58.5	0.18	62%	27%	3.6	68.4	0.16	56%	26%
22-23	1.6	44.5	0.25	50%	20%	1.9	72.5	0.17	39%	18%	5.4	46.2	0.13	66%	29%	1.7	97.4	0.18	60%	27%	3.0	63.7	0.18	62%	27%	2.5	75.2	0.17	56%	25%
23-24						1.6	78.6	0.21	39%	17%	4.8	50.9	0.17	61%	27%						2.9	69.0	0.17	57%	25%	2.4	82.0	0.14	57%	25%
24-25	2.9	52.4	0.21	51%	22%	1.5	85.8	0.20	43%	20%	4.8	56.2	0.17	62%	27%						1.5	73.0	0.20	61%	27%	2.4	91.2	0.15	55%	25%
25-26						1.4	93.4	0.20	41%	18%	4.1	60.0	0.12	69%	30%						1.5	77.0	0.18	62%	27%					
26-27	1.8	58.1	0.23	52%	22%	1.3	105.0	0.24	37%	17%	6.0	67.7	0.14	55%	25%						1.2	80.1	0.16	63%	28%					
27-28											3.6	74.0	0.15	64%	28%						2.5	91.1	0.22	64%	28%					
28-29	1.7	64.2	0.22	49%	20%						2.5	79.7	0.17	53%	24%															
29-30											2.4	87.7	0.19	56%	25%															
30-31	1.5	70.8	0.24	49%	20%						2.1	94.4	0.15	57%	25%															
31-32											1.8	102.4	0.16	53%	24%															
32-33	2.7	85.1	0.20	49%	21%																									
33-34																														
		Mean	0.28	43%	19%			0.21	41%	18%			0.17	59%	26%			0.23	51%	23%			0.21	56%	25%			0.16	56%	25%
		SD	0.18	13%	6%			0.05	6%	3%			0.05	9%	4%			0.10	14%	6%			0.08	12%	5%			0.03	8%	4%

[1]Core SH3-1 was sectioned in 1 cm intervals until a depth of 10 cm; intervals below that depth are 2 cm.

[2]TOC measured via instrumental analysis, except interval 1-2cm which was estimated by (0.4263×OM%) + 0.0097 [Equation 1].

[3] TOC estimated via Equation 1.

4 TOC measured via instrumental analysis for intervals: 0-1, 1-2, 3-4, 6-7, 9-10, 10-11, 12-13, 15-16, 16-17, 18-19, 21-22, 24-24. Remaining intervals estimated via Equation 1.

Table 7. Mean Rates (± 95% C.I.) for all six cores.

Period	Mass Accumulation ($g\ m^{-2}\ yr^{-1}$)	OC Accumulation ($g\ m^{-2}\ yr^{-1}$)	Inorganic Matter Accumulation ($g\ m^{-2}\ yr^{-1}$)	Sediment Accretion[1] ($mm\ yr^{-1}$)
Cumulative[2]	600 (153)	124 (32)	320 (81)	2.79 (0.40)
Pre-2000[3]	494 (85)	114 (19)	234 (56)	2.56 (0.39)
Post-2000	1549 (584)	212 (41)	1086 (556)	4.87 (0.83)

[1] Accretion rates are based on density corrections of depth.

[2] Cumulative errors for Mass, OC, & Inorganic Matter accumulation rates are calculated as an integrated average of standard errors of mass sedimentation for each interval. Errors for Accretion rate are calculated using one standard age error.

[3] Error terms for Pre- & Post-2000 periods are calculated using the standard deviation of the mean rates for adjusted intervals (Figure 2) of each core.

Table 8. Contribution of Coarse OC to Accumulation Rates (g OC m^{-2} yr^{-1})

Core	Age Interval	Fine	Fine & Coarse	Difference
SH3-7	2008-2010	188.9	192.3	3.4
	2005-2008	193.8	197.2	3.3
	2003-2005	222.5	222.8	0.3
	2001-2003	205.8	205.8	0.0
	1996-2001	120.8	121.0	0.2
	1992-1996	142.7	142.7	0.0
	1987-1992	106.8	106.9	0.2
	1984-1987	161.3	161.7	0.5
	1980-1984	126.4	127.5	1.0
	1976-1980	127.6	127.9	0.3
	1972-1976	138.4	139.2	0.8
	1968-1972	95.8	96.1	0.3
	1963-1968	104.1	105.3	1.2
	1961-1963	147.3	149.3	2.0
	1958-1961	131.7	131.8	0.2
	1954-1958	113.8	115.3	1.5
	1949-1954	81.6	82.2	0.5
	1944-1949	89.0	89.2	0.2
	1939-1944	91.4	91.4	0.0
	1933-1939	82.8	100.4	17.6
	1927-1933	79.6	79.8	0.2
	1921-1927	64.6	64.6	0.0
	1913-1921	60.1	60.2	0.1
	Total Period	111.7	113.3	1.62
SH3-8	2008-2010	264.8	267.1	2.3
	2006-2008	257.5	262.8	5.3
	2004-2006	225.6	235.4	9.8
	2000-2004	142.8	144.5	1.7
	1997-2000	152.1	156.1	4.0
	1995-1997	258.5	264.6	6.1
	1993-1995	193.6	198.0	4.4
	1990-1993	202.4	203.7	1.3
	1988-1990	246.3	250.2	3.9
	1986-1988	241.4	243.7	2.3
	1984-1986	254.6	258.1	3.5
	1982-1984	205.8	206.8	1.0
	1979-1982	172.1	176.2	4.1
	1976-1979	196.8	198.6	1.8
	1973-1976	166.5	170.3	3.8
	1971-1973	179.3	182.4	3.2
	1968-1971	169.2	170.9	1.6
	1966-1968	157.9	159.2	1.3
	1963-1966	154.9	155.6	0.7
	1960-1963	152.2	156.5	4.3
	1956-1960	125.1	125.5	0.3
	1952-1956	127.0	127.4	0.5
	1947-1952	95.9	101.1	5.2
	1941-1947	78.0	78.4	0.4
	1937-1941	138.0	140.5	2.5
	1933-1937	120.1	125.1	4.9
	1930-1933	141.8	146.0	4.2
	1919-1930	55.7	56.3	0.6
	Total Period	150.8	153.5	2.7

Table 9. Stable Isotopes and C/N Ratio (Mean ± 1 S.D.) of Intervals.

	SH3-1	SH3-9
δ13C	-27.59 (0.44)	-27.52 (0.36)
δ15N	3.37 (0.84)	3.04 (0.87)
C/N	19.78 (2.29)	22.36 (0.82)

Figures

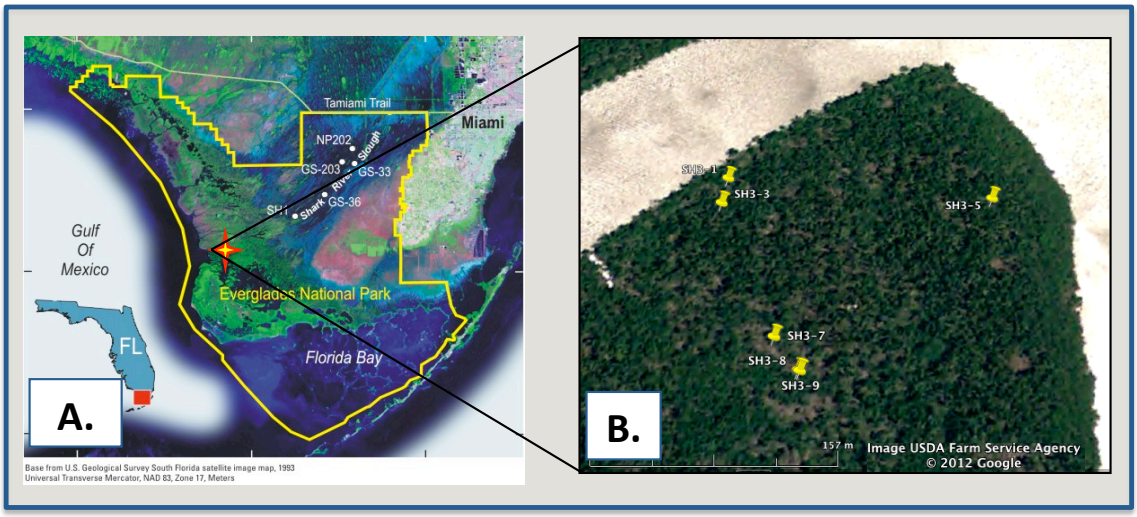

Figure 2. A) Site location on Shark River in SW Everglades. B) Locations of soil cores.

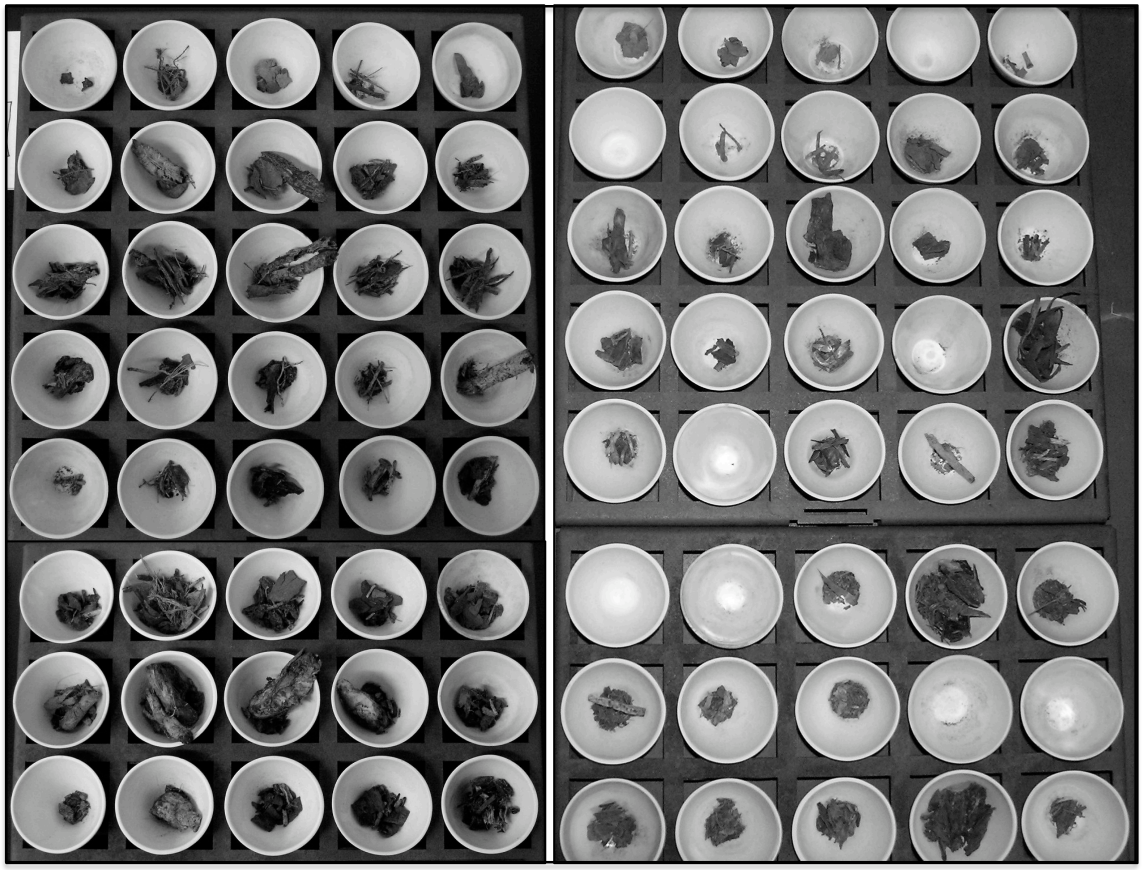

Figure 3. Coarse woody material from SH3-7 (left) and SH3-8 (right). Crucibles are ordered by interval from left to right, top to bottom.

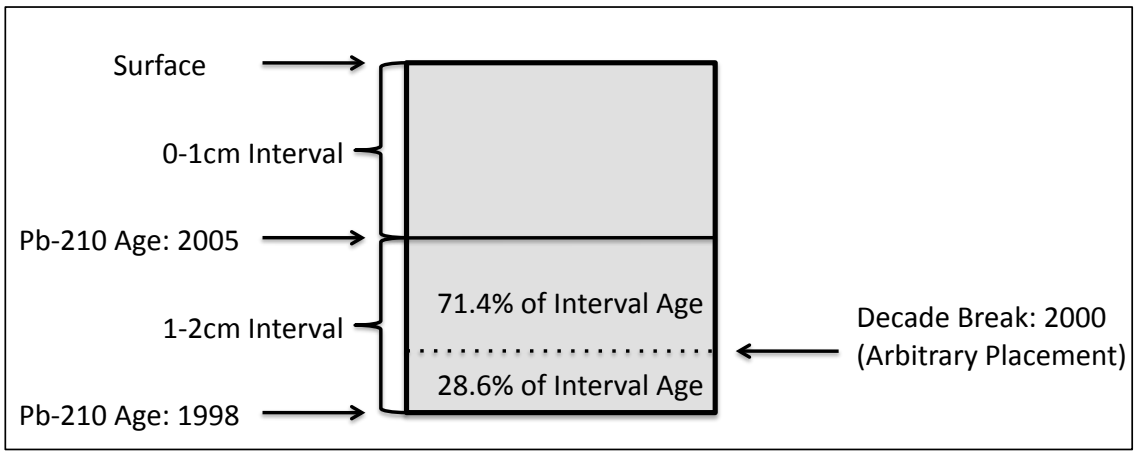

Figure 4. Method for calculating accumulation rates from mid-interval dates.

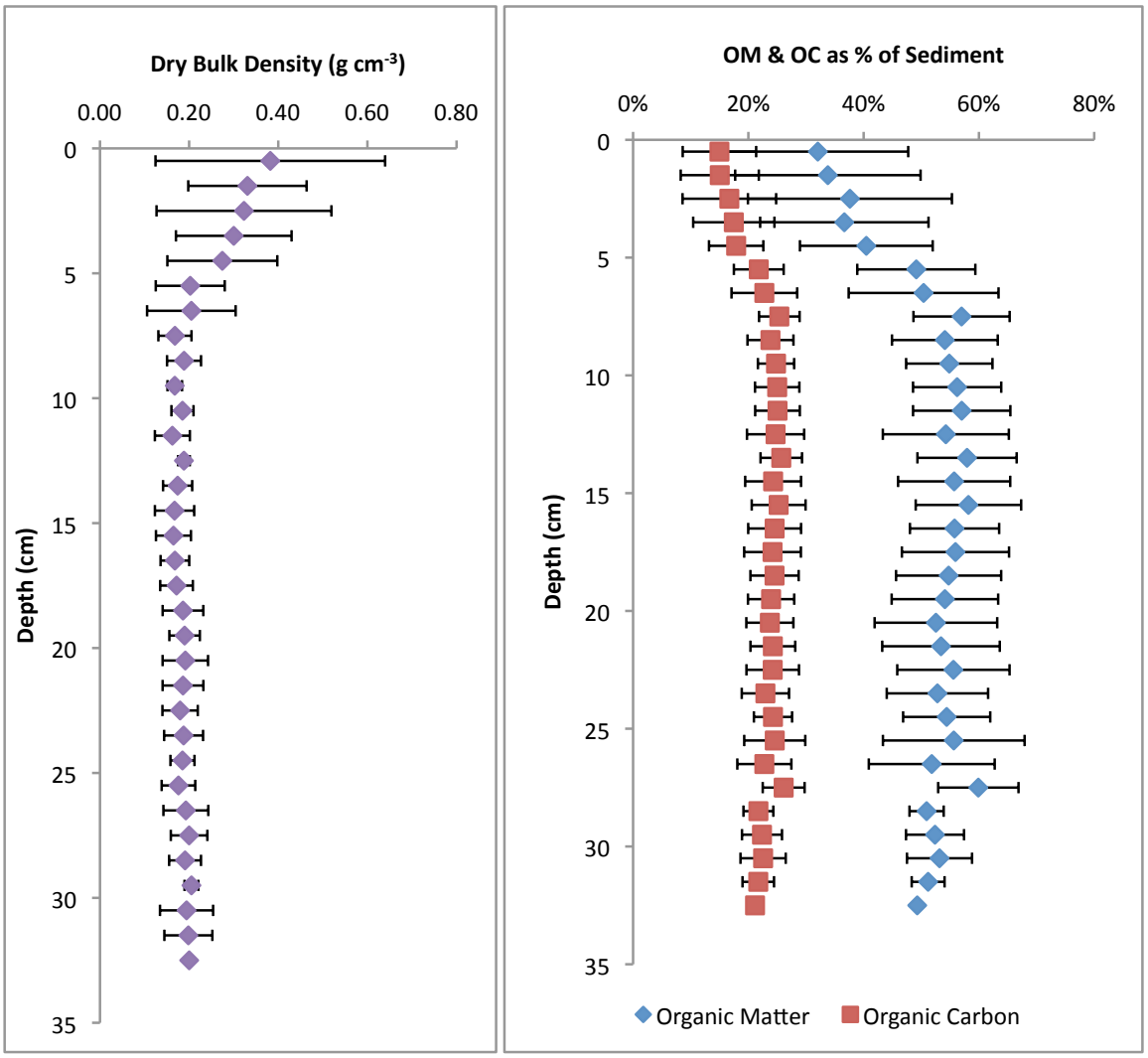

Figure 5. Site values by depth for A. Dry Bulk Density, and B. Organic Matter and Organic Carbon Percentage. Bars represent 1 S.D. Overall site means are: Bulk Density: 0.21 (0.10), OM%: 52% (13%), OC%: 23% (5%).

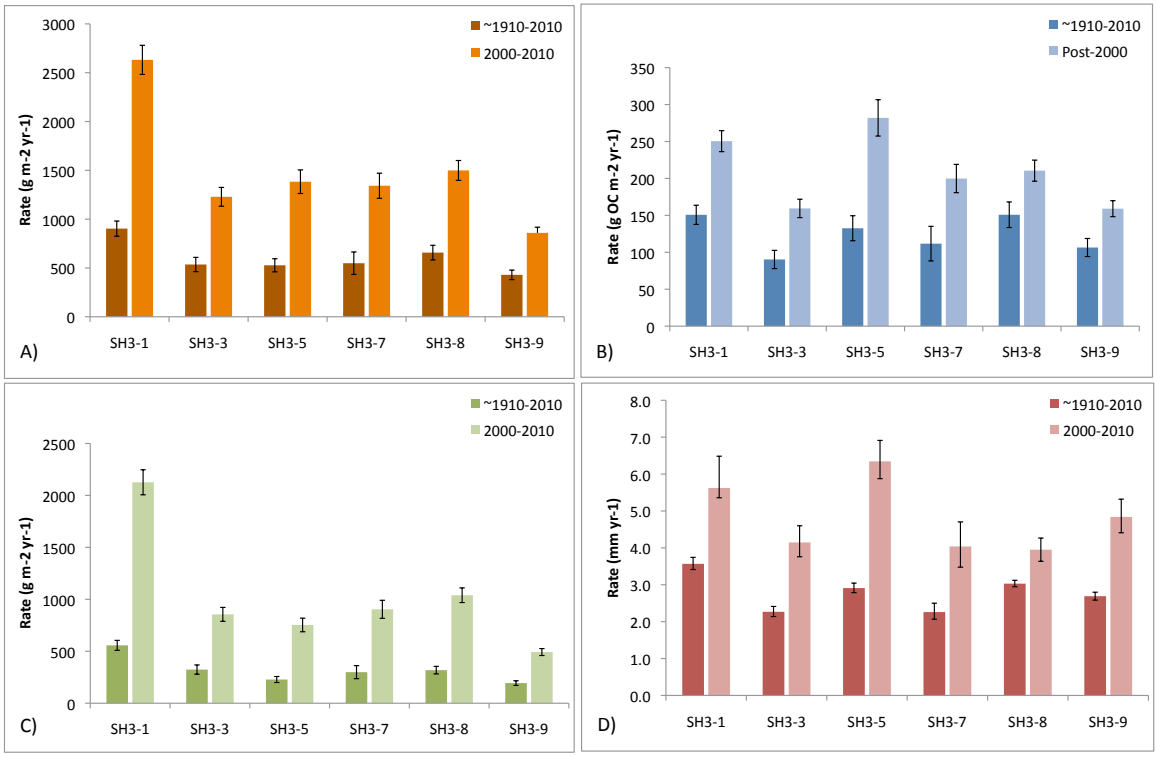

Figure 6. Mean Accumulation Rates by core ± 1 S.E. A) Mass, B) Organic Carbon, C) Inorganic Matter, & D) Soil Accretion. Errors for A, B, & C are calculated as an integrated average of standard errors of mass sedimentation for each interval. Errors for D are calculated from standard age errors.

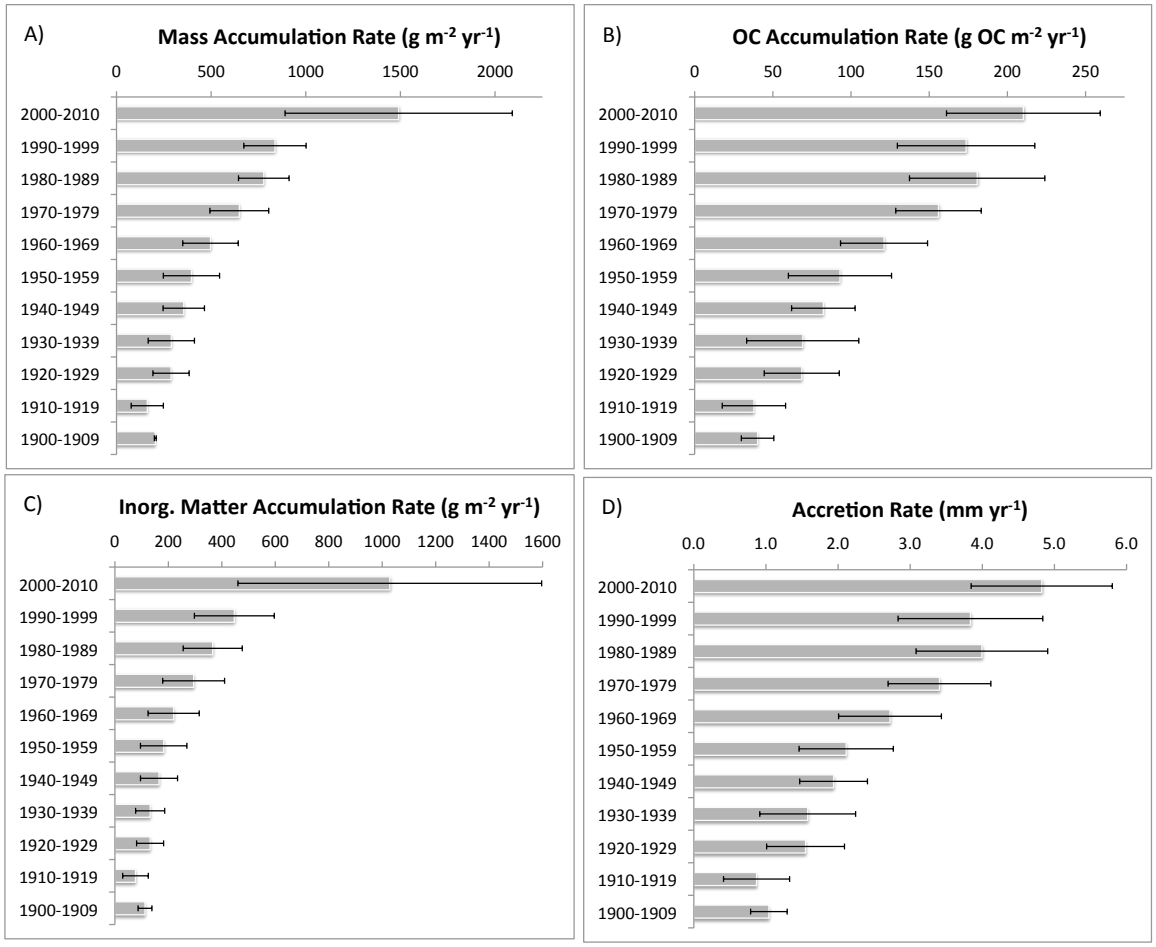

Figure 7. Mean Rates by Decade: A) Mass Accumulation, B) OC Accumulation, C) Inorganic Matter Accumulation, & D) Soil Accretion. Error bars are the standard deviation of the mean rates for adjusted intervals of each core.

List of References

Alongi, D. M. (2011). Carbon payments for mangrove conservation: ecosystem constraints and uncertainties of sequestration potential. *Environmental Science & Policy*, *14*(4), 462-470. Elsevier Ltd. doi:10.1016/j.envsci.2011.02.004

Alongi, D. M., Ayukai, T., Brunskill, G. J., Clough, B. F., & Wolanski, E. (1998). Sources , sinks , and export of organic carbon through a tropical , semi-enclosed delta (Hinchinbrook Channel , Australia). *Mangroves and Salt Marshes*, 237-242.

Alongi, D., Sasekumar, A., Chong, V., & Pfitzner, J. (2004). Sediment accumulation and organic material flux in a managed mangrove ecosystem: estimates of land-ocean-atmosphere exchange in peninsular Malaysia. *Marine geology*, *208*(2-4), 383-402. doi:10.1016/j.margeo.2004.04.016

Alongi, D., Wattayakorn, G., Pfitzner, J., & Tirendi, F. (2001). Organic carbon accumulation and metabolic pathways in sediments of mangrove forests in southern Thailand. *Marine Geology*, *179*(1-2), 85-103. doi:10.1016/S0025-3227(01)00195-5

Amundson, R. (2001). THE CARBON BUDGET IN SOILS. *Annual Review of Earth and Planetary Sciences*, *29*, 535-62.

Appleby, P.G., Oldfield, F., 1992. Application of 210Pb to sedimentation studies. In Ivanovich, M. , Harmon, R.S. (eds) Uranium-series Disequilibrium: Applications to Earth, Marine & Environmental Sciences. Oxford University Press. Oxford: 731-778.

Appleby, P. G., & Oldfield, F. (1978). The Calculation of Lead-210 Dates Assuming A Constant Rate of Supply of Unsupported ^{210}Pb to the Sediment. *Catena*, *5*.

Baldocchi, D., Falge, E., Gu, L., Olson, R., Hollinger, D., Running, S., Anthoni, P., et al. (2001). FLUXNET: A New Tool to Study the Temporal and Spatial Variability of Ecosystem–Scale Carbon Dioxide, Water Vapor, and Energy Flux Densities. *Bulletin of the American Meteorological Society*, *82*(11), 2415-2434. doi:10.1175/1520-0477(2001)082<2415:FANTTS>2.3.CO;2

Barr, J. G., Engel, V., Fuentes, J. D., Zieman, J. C., O'Halloran, T. L., Smith, T. J., & Anderson, G. H. (2010). Controls on mangrove forest-atmosphere carbon dioxide exchanges in western Everglades National Park. *Journal of Geophysical Research*, *115*(G2), 1-14. doi:10.1029/2009JG001186

Barr, J. G., Engel, V., Smith, T. J., & Fuentes, J. D. (2011). Hurricane disturbance and recovery of energy balance, CO2 fluxes and canopy structure in a mangrove forest of the Florida Everglades. *Agricultural and Forest Meteorology*. Elsevier B.V. doi:10.1016/j.agrformet.2011.07.022

Bouillon, S, Connolly, R., & Lee, S. (2008a). Organic matter exchange and cycling in mangrove ecosystems: Recent insights from stable isotope studies. *Journal of Sea Research*, *59*(1-2), 44-58. doi:10.1016/j.seares.2007.05.001

Bouillon, Steven, Borges, A. V., Castañeda-Moya, E., Diele, K., Dittmar, T., Duke, N. C., Kristensen, E., et al. (2008b). Mangrove production and carbon sinks: A revision of global budget estimates. *Global Biogeochemical Cycles*, *22*(2), 1-12. doi:10.1029/2007GB003052

Breithaupt, J. L., Smoak, J.M., Smith III, T.J., Sanders, C.J., and Hoare, A. (Submitted to Global Biogeochemical Cycles March 2012). Organic Carbon Burial Rates in Mangrove Sediments: Strengthening the Global Budget.

Brunskill, G. (2002). Carbon Burial Rates in Sediments and a Carbon Mass Balance for the Herbert River Region of the Great Barrier Reef Continental Shelf, North Queensland, Australia. *Estuarine, Coastal and Shelf Science*, *54*(4), 677-700. doi:10.1006/ecss.2001.0852

Callaway, J., DeLaune, R., & Patrick Jr, W. (1997). Sediment accretion rates from four coastal wetlands along the Gulf of Mexico. *Journal of Coastal Research*, *13*(1), 181–191. JSTOR.

Castañeda-Moya, E., Twilley, R. R., Rivera-Monroy, V. H., Marx, B. D., Coronado-Molina, C., & Ewe, S. M. L. (2011). Patterns of Root Dynamics in Mangrove Forests Along Environmental Gradients in the Florida Coastal Everglades, USA. *Ecosystems*. doi:10.1007/s10021-011-9473-3

Castañeda-Moya, E., Twilley, R. R., Rivera-Monroy, V. H., Zhang, K., Davis, S. E., & Ross, M. (2009). Sediment and Nutrient Deposition Associated with Hurricane Wilma in Mangroves of the Florida Coastal Everglades. *Estuaries and Coasts*, *33*(1), 45-58. doi:10.1007/s12237-009-9242-0

Chen, R., & Twilley, R. R. (1999). A simulation model of organic matter and nutrient accumulation in mangrove wetland soils. *Biogeochemistry*, *44*(1), 93-118. doi:10.1007/BF00993000

Childers, D., Boyer, J., Davis, S., & Madden, C. (2006). Relating precipitation and water management to nutrient concentrations in the oligotrophic “upside-down” estuaries of the Florida Everglades. *Limnology and Oceanography*, *51*, 602-616.

Chmura, G. L., Anisfeld, S. C., Cahoon, D. R., & Lynch, J. C. (2003). Global carbon sequestration in tidal, saline wetland soils. *Global Biogeochemical Cycles*, *17*(4). doi:10.1029/2002GB001917

Davidson, E. a, & Janssens, I. a. (2006). Temperature sensitivity of soil carbon decomposition and feedbacks to climate change. *Nature*, *440*(7081), 165-73. doi:10.1038/nature04514

De Deyn, G. B., Cornelissen, J. H. C., & Bardgett, R. D. (2008). Plant functional traits and soil carbon sequestration in contrasting biomes. *Ecology letters*, *11*(5), 516-31. doi:10.1111/j.1461-0248.2008.01164.x

Donato, D. C., Kauffman, J. B., Murdiyarso, D., Kurnianto, S., Stidham, M., & Kanninen, M. (2011). Mangroves among the most carbon-rich forests in the tropics. *Nature Geoscience*, *4*(5), 293-297. Nature Publishing Group. doi:10.1038/ngeo1123

Duarte, C. M., Middelburg, J. J., & Caraco, N. (2005). Major role of marine vegetation on the oceanic carbon cycle. *Biogeosciences*, *2*(1), 1-8. doi:10.5194/bg-2-1-2005

Duarte, Carlos M., & Cebrián, J. (1996). The fate of marine autotrophic production. *Limnology and Oceanography*, *41*(8), 1758-1766. doi:10.4319/lo.1996.41.8.1758

Fourqurean, J. W., Zieman, J. C., & Powell, G. V. N. (1992). Phosphorus limitation of primary production in Florida Bay: Evidence from C:N:P ratios of the dominant seagrass Thalassia testudinum. *Limnology and Oceanography*, *37*(1), 162-171. doi:10.4319/lo.1992.37.1.0162

Furukawa, K., & Wolanski, E. (1996). Sedimentation in mangrove forests. *Mangroves and Salt Marshes*, 1(1), 3-10.

Hovmand, M. F., Nielsen, S. P., & Johnsen, I. (2009). Root uptake of lead by Norway spruce grown on 210Pb spiked soils. *Environmental pollution (Barking, Essex : 1987)*, *157*(2), 404-9. Elsevier Ltd. doi:10.1016/j.envpol.2008.09.038

Krauss, K. W., Doyle, T. W., Twilley, R. R., Rivera-Monroy, V. H., & Sullivan, J. K. (2006). Evaluating the relative contributions of hydroperiod and soil fertility on growth of south Florida mangroves. *Hydrobiologia*, *569*(1), 311-324. doi:10.1007/s10750-006-0139-7

Kristensen, E. (2008). Mangrove crabs as ecosystem engineers; with emphasis on sediment processes. *Journal of Sea Research*, *59*(1-2), 30-43. doi:10.1016/j.seares.2007.05.004

Kristensen, Erik, Bouillon, S., Dittmar, T., & Marchand, C. (2008). Organic carbon dynamics in mangrove ecosystems: A review. *Aquatic Botany*, *89*(2), 201-219. doi:10.1016/j.aquabot.2007.12.005

Lynch, J. C. (1989). *Sedimentation and nutrient accumulation in mangrove ecosystems of the Gulf of Mexico*. University of Southwestern Louisiana, Lafayette, LA.

Lynch, J., Meriwether, J., McKee, B., Vera-Herrera, F., & Twilley, R. (1989). Recent accretion in mangrove ecosystems based on 137 Cs and 210 Pb. *Estuaries*, *12*(4).

Mcleod, E., Chmura, G. L., Bouillon, S., Salm, R., Björk, M., Duarte, C. M., Lovelock, C. E., et al. (2011). A blueprint for blue carbon: toward an improved understanding of the role of vegetated coastal habitats in sequestering CO 2. *Frontiers in Ecology and the Environment*, 110621060659096. doi:10.1890/110004

NOAA National Ocean Service: http://tidesandcurrents.noaa.gov/sltrends/sltrends_station.shtml?stnid=8724580

Noe, G. B., Childers, D. L., & Jones, R. D. (2001). Phosphorus Biogeochemistry and the Impact of Phosphorus Enrichment: Why Is the Everglades so Unique? *Ecosystems*, *4*(7), 603-624. doi:10.1007/s10021-001-0032-1

Romigh, M. M., Davis, S. E., Rivera-Monroy, V. H., & Twilley, R. R. (2006). Flux of organic carbon in a riverine mangrove wetland in the Florida Coastal Everglades. *Hydrobiologia*, *569*(1), 505-516. doi:10.1007/s10750-006-0152-x

Sanders, C. J., Smoak, J. M., Sanders, L. M., Sathy Naidu, a., & Patchineelam, S. R. (2010). Organic carbon accumulation in Brazilian mangal sediments. *Journal of South American Earth Sciences*, *30*(3-4), 189-192. Elsevier Ltd. doi:10.1016/j.jsames.2010.10.001

Sanders, C. J., Smoak, J. M., Waters, M. N., Sanders, L. M., Brandini, N., & Patchineelam, S. R. (2012). Organic matter content and particle size modifications in mangrove sediments as responses to sea level rise. *Marine environmental research*. doi:10.1016/j.marenvres.2012.02.004

Smith, J., Boto, K. G., & Giddins, L. (1991). Keystone Species and Mangrove Forest Dynamics : the Influence of Burrowing by Crabs on Soil Nutrient Status and Forest Productivity, *Estuarine, Coastal and Shelf Science*, (537), 419-432.

Smith, T.J., Anderson, G. H., Balentine, K., Tiling, G., Ward, G. A., & Whelan, K. R. T. (2009). Cumulative impacts of hurricanes on Florida mangrove ecosystems: sediment deposition, storm surges and vegetation. *Wetlands*, *29*(1), 24–34. Springer. doi:10.1672/08-40.1

Smith, Thomas J, Robblee, M. B., Wanless, H. R., Doyle, T. W., Im, T. J. S., & Florida, S. (2010). Hurricanes, Mangroves, and Lightning Strikes. *Sciences-New York*, *44*(4), 256-262.

Smoak, J.M., Breithaupt, J. L., Smith III, T.J., & Sanders, C.J. (Submitted to Catena December 2011). Sediment accretion and organic carbon burial relative to sea-level rise and storm events in two mangrove forests in Everglades National Park.

Twilley, R., Chen, R., & Hargis, T. (1992). Carbon Sinks in Mangroves and their Implications to Carbon Budget of Tropical Coastal Ecosystems. *Water, Air, & Soil Pollution*, *64*(1), 265–288. Springer.

Whelan, Kevin R. T., Smith, T. J., Anderson, G. H., & Ouellette, M. L. (2009). Hurricane Wilma's Impact on Overall Soil Elevation and Zones Within the Soil Profile in a Mangrove Forest. *Wetlands*, *29*(1), 16-23. doi:10.1672/08-125.1

Whelan, Kevln R T, Smith, T. J., Cahoon, D. R., Geological, U. S., International, F., Ehan, O., Reseat, P. W., et al. (2005). Groundwater Control of Mangrove Surface Elevation : Shrink and Swell Varies with Soil Depth. Estuaries, 28(6), 833-843.